Insulators and metals with topological order
and discrete symmetry breaking

Shubhayu Chatterjee[1] and Subir Sachdev[1, 2]

[1]*Department of Physics, Harvard University, Cambridge MA 02138, USA*
[2]*Perimeter Institute for Theoretical Physics,*
Waterloo, Ontario, Canada N2L 2Y5

(Dated: February 28, 2017)

Abstract

Numerous experiments have reported discrete symmetry breaking in the high temperature pseudogap phase of the hole-doped cuprates, including breaking of one or more of lattice rotation, inversion, or time-reversal symmetries. In the absence of translational symmetry breaking or topological order, these conventional order parameters cannot explain the gap in the charged fermion excitation spectrum in the anti-nodal region. Zhao *et al.* (Nature Physics **12**, 32 (2016)) and Jeong *et al.* (Nature Communications **8**, 15119 (2017)) have also reported inversion and time-reversal symmetry breaking in insulating Sr_2IrO_4 similar to that in the metallic cuprates, but co-existing with Néel order. We extend an earlier theory of topological order in insulators and metals, in which the topological order combines naturally with the breaking of these conventional discrete symmetries. We find translationally-invariant states with topological order co-existing with both Ising-nematic order and spontaneous charge currents. The link between the discrete broken symmetries and the topological-order-induced pseudogap explains why the broken symmetries do not survive in the confining phases without a pseudogap at large doping. Our theory also connects to the O(3) non-linear sigma model and $\mathbb{CP}^1$ descriptions of quantum fluctuations of the Néel order. In this framework, the optimal doping criticality of the cuprates is primarily associated with the loss of topological order.

I. INTRODUCTION

Experimental studies of the enigmatic high temperature 'pseudogap' regime of the hole-doped cuprate compounds have reported numerous possible discrete symmetry breaking order parameters.[1–13] There is evidence for lattice rotation symmetry breaking, interpreted in terms of an Ising-nematic order,[14] and for one or both of inversion and time-reversal symmetry breaking, usually interpreted in terms of Varma's current loop order.[15–17] Both of these orders have the full translational symmetry of the square lattice, and cannot, by themselves, be responsible for gap in the charged fermionic spectrum near the 'anti-nodal' points ($(\pi, 0)$ and $(0, \pi)$) of the square lattice Brillouin zone.

An interesting and significant recent development has been the observation of inversion[11] and time-reversal[13] symmetry breaking in the iridate compound $Sr_2Ir_{1-x}Rh_xO_4$; Ref. 18 has shown that this iridate is described by a one-band Hubbard model very similar to that for the cuprates. The inversion symmetry breaking is strongest in the insulator at $x = 0$ where it co-exists with Néel order; at non-zero x, both orders persist, but the discrete order is present at higher temperatures. Motivated by the similarities in the light and neutron scattering signatures between the cuprate and iridate compounds, we will present here a common explanation based upon the quantum fluctuations of antiferromagnetism.

Long-range Néel order (which breaks translational symmetry) can clearly be the origin of a gap in the charged fermionic spectrum at the anti-nodes. In the traditional spin density wave theory of the quantum fluctuations of the Néel order,[19] there is a transition to a state without Néel order, with full translational symmetry, a large Fermi surface, and no anti-nodal gap. However, the anti-nodal gap can persist into the non-Néel phase[20] when the resulting phase has topological order[21–25] (see footnote[26] for the precise definition of topological order, and the review in Ref. 27). We shall use topological order as the underlying mechanism for the pseudogap. Moreover, early studies of spin liquid insulators with $\mathbb{Z}_2$ topological order showed that there can be a non-trivial interplay between topological order and the breaking of conventional discrete symmetries. The $\mathbb{Z}_2$ spin liquid obtained in Refs. 28 and 29 co-existed with Ising-nematic order: this was a consequence of the p-wave pairing of bosonic spinons. A similar interplay with time-reversal and inversion symmetries was discussed by Barkeshli $et\ al.$,[30] using higher angular momentum pairing of fermionic spinons. Here we shall use the formalism of Refs. 27, 31, and 32 to generalize the state[28,29] with $\mathbb{Z}_2$ topological order to also allow for the breaking of inversion and time-reversal symmetries, both in the insulator and the metal. We will find states with spontaneous charge currents (see Fig. 2) and topological order, one of which (Fig. 2a) also has the Ising-nematic order observed in experiments.[1,3,6,8]

The association between topological order and discrete broken symmetries implies that the broken symmetries will not be present in the confining phases at larger doping. This is an important

advantage of our approach over more conventional excitonic condensation theories of broken symmetries. In the latter approaches there is no strong reason to connect the disappearance of the pseudogap with vanishing of the symmetry order parameter.

We will begin in Section II by a semi-classical treatment of the quantum fluctuations of antiferromagnetism[33–35] using the O(3) non-linear sigma model. In the insulator, this approach has been successfully used to describe the thermal fluctuations of the Néel order, and also the adjacent quantum phase without Néel order; the latter was argued to have valence bond solid (VBS) order,[36,37] and is accessed across a deconfined quantum critical point.[38,39] Here, we will identify an order parameter, $\boldsymbol{O}$, for inversion and time-reversal symmetry breaking in terms of the fields of the O(3) sigma model.

It is also useful to formulate the semi-classical treatment using the $\mathbb{CP}^1$ model for bosonic, fractionalized spinons coupled to a U(1) gauge field. In these terms, an order parameter $\boldsymbol{O}$ for inversion and time-reversal symmetry breaking turns out to be the cross product of the emergent U(1) electric and magnetic fields. The $\mathbb{CP}^1$ formulation yields an effective gauge theory, in Eq. (2.8) for quantum phases with spontaneous charge currents, but without Néel order.

Formally, a model expressed in terms of spins alone has no charge fluctuations, and so has vanishing electromagnetic charge current, $\boldsymbol{J} = 0$. However, in practice, every spin model arises from an underlying Hubbard-like model, in which states suppressed by the on-site repulsion U are eliminated by a canonical transformation. If we undo this canonical transformation, we can expect that a suitable multi-spin operator will induce a non-zero $\boldsymbol{J}$ at some order in the $1/U$ expansion. As $\boldsymbol{O}$ has the same symmetry signature as $\boldsymbol{J}$, we can expect that a state with $\langle\boldsymbol{O}\rangle$ non-zero will also have $\langle\boldsymbol{J}(\boldsymbol{r})\rangle$ non-zero. We will examine states in which $\langle\boldsymbol{O}\rangle$ is independent of $\boldsymbol{r}$ in the continuum limit, so that translational symmetry is preserved. However, by Bloch's theorem,[40,41] we must have

$$\int d^2r \langle\boldsymbol{J}(\boldsymbol{r})\rangle = 0, \tag{1.1}$$

and so $\boldsymbol{J}$ cannot be $\boldsymbol{r}$ independent. If we want to preserve translational symmetry, the resolution is that there will be intra-unit cell variations in $\langle\boldsymbol{J}(\boldsymbol{r})\rangle$ to retain compatibility with Bloch's theorem. In a tight-binding model with one site per unit cell, we label each unit cell by a site label, i, and a link label ρ so that the combination (i, ρ) identifies the complete set of lattice links, with no double counting. So from each lattice site i, there are set of vectors $\boldsymbol{v}_\rho$ connecting i to its neighboring sites, and both $\boldsymbol{v}_\rho$ and $-\boldsymbol{v}_\rho$ are not members of this set: see Fig. 1. In this setup, Bloch's theorem states that

$$\sum_\rho \langle\boldsymbol{J}_\rho\rangle = 0. \tag{1.2}$$

where $\boldsymbol{J}_\rho$ is the current along the $\boldsymbol{v}_\rho$ direction. Note that Eq. (1.2) is a stronger statement than current conservation because the sum over ρ does not include all links connected to site i, only
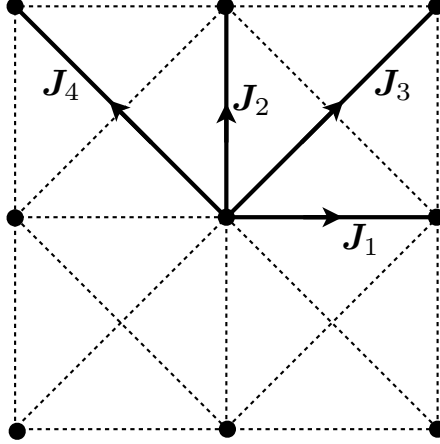
3

FIG. 1. Definitions of currents on the square lattice with first and second neighbor hopping. The filled circles are the sites of the Cu atoms in the cuprates. Shown above are the 4 currents J_ρ from the central lattice site. These currents obey Eq. (1.2) when the translational symmetry of the square lattice is preserved.

half of them. Eq. (1.2) is equivalent to the statement that there are current 'loops', and these are clearly possible even in a single-band model.[42,43] In the presence of a $\boldsymbol{r}$-independent $\boldsymbol{O}$ condensate, we can write by symmetry that (to linear order in the broken symmetry)

$$\langle J_{\rho p} \rangle = K^\rho_{pp'} \langle O_{p'} \rangle , \tag{1.3}$$

where $p, p' = x, y$ are spatial indices, and $K^\rho_{pp'}$ is a response function obtained in the $1/U$ expansion which respects all square lattice symmetries. Compatibility with Bloch's theorem requires that

$$\sum_\rho K^\rho_{ij} = 0, \tag{1.4}$$

and there are no conditions on the value of $\langle \boldsymbol{O} \rangle$.

We will turn to an explicit treatment of the charged excitations, and a computation of $\boldsymbol{J}_\rho$ in Section III: our results there do obey Eqs. (1.1) and (1.4). Section III will present a lattice formulation in which the U(1) gauge field of the $\mathbb{CP}^1$ model is embedded in a SU(2) lattice gauge theory.[27,31,32,44] This lattice gauge theory has the advantage of including all Berry phases and charged fermionic excitations, and also for allowing an eventual transition into a conventional Fermi liquid state at high enough doping. Our interest here will be in insulating and metallic states at lower doping, which have topological order and a gap to charged fermionic excitations in the anti-nodal region. At the same time we shall show that, with an appropriate effective action, there can be a background modulated gauge flux under which *gauge-invariant* observables remain
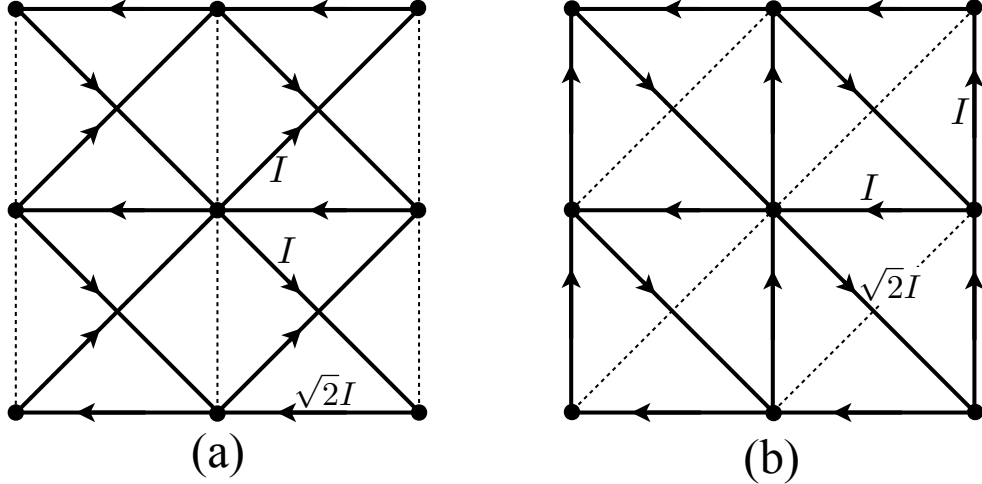
4

FIG. 2. Currents on the links in two classes of states with broken time reversal and inversion symmetries. The states have the full translational symmetry of the square lattice, and the magnitude of the current is noted on some links. The current vanishes on the dashed lines. In (a), the currents have the magnitudes $|\boldsymbol{J}_1| = \sqrt{2}I$, $|\boldsymbol{J}_2| = 0$, $|\boldsymbol{J}_3| = I$, $|\boldsymbol{J}_4| = I$, and the order parameter $\boldsymbol{O} \sim (-1,0)$. In (b), the currents have the magnitudes $|\boldsymbol{J}_1| = I$, $|\boldsymbol{J}_2| = I$, $|\boldsymbol{J}_3| = 0$, $|\boldsymbol{J}_4| = \sqrt{2}I$, and the order parameter $\boldsymbol{O} \sim (1,-1)$. The state in (a) has Ising-nematic order $\mathcal{N}_1$ non-zero, while the state in (b) has Ising-nematic order $\mathcal{N}_2$ non-zero (see Eq. (1.5)). Experiments on the cuprates[1,3,6,8] observe the Ising-nematic order $\mathcal{N}_1$.

translationally invariant but break one or more of inversion, time-reversal and lattice rotation symmetries. Our computations will demonstrate the presence of spontaneous charge currents obeying Eq. (1.2) in states which break both inversion and time-reversal, but preserve translation. The two classes of spontaneous current patterns we find are shown in Fig. 2. Note that the product of time-reversal and inversion is preserved in these states. The state in Fig. 2a has $\langle \boldsymbol{O} \rangle \sim (-1,0)$, while the state in Fig. 2b has $\langle \boldsymbol{O} \rangle \sim (1,-1)$. Both states belong to separate quartets of equivalent states (with $\langle \boldsymbol{O} \rangle \sim (\pm 1, 0), (0, \pm 1)$ and $\langle \boldsymbol{O} \rangle \sim (\pm 1, \pm 1)$) which can be obtained from them by symmetry operations. Both states also break an Ising-nematic symmetry. In general, on the square lattice, we can define two Ising-nematic order parameters, which are invariant under both inversion and time-reversal, but not under lattice rotation symmetries. In terms of $\boldsymbol{O}$, these order parameters are

$$\mathcal{N}_1 = O_x^2 - O_y^2 \quad , \quad \mathcal{N}_2 = O_x O_y. \tag{1.5}$$

The state in Fig. 2a has only $\langle \mathcal{N}_1 \rangle \neq 0$, while the state in Fig. 2b has only $\langle \mathcal{N}_2 \rangle \neq 0$. We note that the state in Fig. 1b of Simon and Varma[16] in a two band model has the same symmetry as the state in our Fig. 2b, and also the spontaneous current states considered in Refs. 42 and 43. The state in our Fig. 2a appears to not have been considered earlier: it has the same Ising-nematic

	$\mathcal{T}$	T_x	T_y	I_x	I_y
$\vec{n}$	$-$	$-$	$-$	$+$	$+$
$\vec{L}$	$-$	$+$	$+$	$+$	$+$
e_x	$+$	$-$	$-$	$-$	$+$
e_y	$+$	$-$	$-$	$+$	$-$
b	$-$	$-$	$-$	$-$	$-$
J_x	$-$	$+$	$+$	$-$	$+$
J_y	$-$	$+$	$+$	$+$	$-$

TABLE I. Symmetry signatures of various fields under time reversal ($\mathcal{T}$), translation by a square lattice spacing along the x (T_x) and y (T_y) directions, and reflections about a square lattice site involving $x \to -x$ (I_x) or $y \to -y$ (I_y).

order observed in experiments in the cuprates.[1,3,6,8]

Finally, we note that our results are also easily extended to states with long-range antiferromagnetic order by condensing the spectator bosonic spinons.

II.   O(3) NON-LINEAR SIGMA AND $\mathbb{CP}^1$ MODELS

The familiar O(3) model describes quantum fluctuations of the unit vector $\vec{n}(\boldsymbol{r}, \tau)$, representing the local antiferromagnetic order, with action over space, $\boldsymbol{r}$, and imaginary time τ

$$\mathcal{S}_{\vec{n}} = \frac{1}{2g} \int d^2 r d\tau \, (\partial_\mu \vec{n})^2 \,, \tag{2.1}$$

where μ extends over the 3 spacetime indices, and g is a coupling constant. For our purposes, we need the symmetry transformation properties of the operator $\vec{n}$ and its canonically conjugate angular momentum $\vec{L}$; the latter is also interpreted as the conserved ferromagnetic moment.[34] We list these transformations properties in Table I.

Table I also shows the symmetry transformations of charge current $\boldsymbol{J}$. Formally, a model expressed in terms of spins alone has no charge fluctuations, and so we will have $\boldsymbol{J} = 0$. However, in practice, every spin model arises from an underlying Hubbard-like model, in which states suppressed by the on-site repulsion U are eliminated by a canonical transformation. If we undo this canonical transformation, we can expect that a suitable multi-spin operator will couple linearly to $\boldsymbol{J}$ at some order in the $1/U$ expansion; naturally, we need this multi-spin operator to have the same symmetry signature as $\boldsymbol{J}$. We therefore use Table I to find the simplest such combination of

6

$\vec{n}$ and $\vec{L}$; the needed operator turns out to be

$$\boldsymbol{O} = \vec{L} \cdot (\vec{n} \times \boldsymbol{\nabla}\vec{n}). \tag{2.2}$$

We will therefore be interested in states in which $\langle \boldsymbol{O} \rangle$ is non-zero and independent of $\boldsymbol{r}$. In magnetically ordered states, $\langle \boldsymbol{O} \rangle$ is non-zero for a 'canted spiral' in which the spins precess around the base of a cone along a fixed spatial direction:[45] a non-zero $\vec{n} \times \boldsymbol{\nabla}\vec{n}$ corresponds to a spin spiral, which must cant to introduce a non-zero $\vec{L}$. However, our interest here is in states in which $\langle \boldsymbol{O} \rangle$ is non-zero without long-range magnetic order, in which $\langle \vec{n} \rangle = 0$ and $\langle \vec{L} \rangle = 0$. For example, we can add to $S_{\vec{n}}$ an effective potential $V(\boldsymbol{O})$ which is invariant under all symmetries, and a suitable $V(\boldsymbol{O})$ will induce an $\boldsymbol{O}$ condensate. In Section III, we will present specific lattice models for which such condensates arise. In any such state with an $\boldsymbol{O}$ condensate, we can also expect that $\langle \boldsymbol{J}(\boldsymbol{r}) \rangle$ is also non-zero, and obeys Eqs. (1.3) and (1.4).

Let us now turn to the $\mathbb{CP}^1$ model. This is expressed in terms of bosonic spinons, z_α, with $\alpha = \uparrow, \downarrow$ and $|z_\uparrow|^2 + |z_\downarrow|^2 = 1$, related to the antiferromagnetic order by

$$\vec{n} = z_\alpha^* \vec{\sigma}_{\alpha\beta} z_\beta, \tag{2.3}$$

where $\vec{\sigma}$ are the Pauli matrices. The action for the $\mathbb{CP}^1$ model has an emergent U(1) gauge field $a_\mu = (a_\tau, \boldsymbol{a})$:

$$\mathcal{S}_z = \frac{1}{g} \int d^2r d\tau \, |(\partial_\mu - ia_\mu)z_\alpha|^2. \tag{2.4}$$

We define the associated emergent electric and magnetic fields by, as usual by

$$\boldsymbol{e} = \partial_\tau \boldsymbol{a} - \boldsymbol{\nabla}a_\tau \quad , \quad b = \hat{\boldsymbol{z}} \cdot (\boldsymbol{\nabla} \times \boldsymbol{a}), \tag{2.5}$$

where $\hat{\boldsymbol{z}}$ is a unit vector orthogonal to the square lattice in the x-y plane. These gauge-invariant fields are connected to the topological charge of the O(3) order parameter $\vec{n}$ via

$$\boldsymbol{e} = \frac{1}{2}\vec{n} \cdot (\partial_\tau \vec{n} \times \boldsymbol{\nabla}\vec{n}) \quad , \quad b = \frac{1}{2}\vec{n} \cdot (\partial_x \vec{n} \times \partial_y \vec{n}). \tag{2.6}$$

We can now use (2.6) to deduce the symmetry signatures of $\boldsymbol{e}$ and b, and the results were shown in Table I. Finally, as in the O(3) formulation, we now search for a combination of $\boldsymbol{e}$ and b which has the same symmetry signature as the charge current; the simplest possibility is

$$\boldsymbol{O} = \boldsymbol{e} \times (b\,\hat{\boldsymbol{z}}). \tag{2.7}$$

Note that the operators in Eqs. (2.2) and (2.7) are not equal to each other: they are distinct representations with the same symmetry signature. The connection between $\boldsymbol{O}$ and the charge current $\boldsymbol{J}$ in Eq. (1.3) also applies to Eq. (2.7). Also at this order, $\boldsymbol{O}$ is equal to the conserved

Poynting vector of the gauge field, but we do not expect possible higher order terms in $\boldsymbol{O}$ to yield a conserved quantity. Also, as for the O(3) model, we can add a suitable potential $V(\boldsymbol{O})$ to the $\mathbb{CP}^1$ action $\mathcal{S}_z$ in Eq. (2.4) and induce a phase with an $\boldsymbol{O}$ condensate.

The advantage of the $\mathbb{CP}^1$ formulation is that we can now write down an effective action for the phase without Néel order, where the z_α spinons are gapped. We integrate out the z_α spinons and generate an effective action for the U(1) gauge field a_μ in the state where $\boldsymbol{O}$ is condensed; using gauge invariance and symmetries, the imaginary time action has the form

$$\mathcal{S}_a = \int d^2r d\tau \left[\frac{\gamma_1}{2} (\partial_\tau a_i - \partial_i a_\tau)^2 + \frac{\gamma_2}{2} (\partial_x a_y - \partial_y a_x)^2 + i\Gamma_i (\partial_\tau a_i - \partial_i a_\tau)(\partial_x a_y - \partial_y a_x) \right], \quad (2.8)$$

where $\gamma_{1,2}$ are coupling constants. The novel feature is the last term which has a co-efficient proportional to $\langle \boldsymbol{O} \rangle$

$$\boldsymbol{\Gamma} \propto \hat{\boldsymbol{z}} \times \langle \boldsymbol{O} \rangle; \quad (2.9)$$

this term leads to a relatively innocuous modification of the gauge field propagator from the familiar relativistic form. By itself, the U(1) gauge theory $\mathcal{S}_a$ is unstable to confinement by the proliferation of monopoles and the appearance of VBS order.[36] However, topological order can be stabilized if there are Fermi surfaces of U(1) charged fermions[46,47] which suppress monopoles. Alternatively, $\mathbb{Z}_2$ topological order can be stabilized[28,29,48] by condensing a Higgs scalar with U(1) charge 2. We will meet both mechanisms in the model of Section III. The resulting state has co-existing topological order and spontaneous charge currents.

III. SU(2) LATTICE GAUGE THEORY

This section will extend the SU(2) gauge theory of Refs. 27, 31, 32, and 44 to obtain lattice model realizations of the physics sketched in Section II. The SU(2) gauge theory was initially proposed as a convenient reformulation of particular theories of topological order in insulators[28,29,36,37] and metals,[47,49,50] which also allowed one to recover the large Fermi surface Fermi liquid at large doping. For our purposes, it also turns out to be a convenient setting in which to realize the states discussed in Section II. The theory explicitly includes charged fermionic excitations, and so it is possible to obtain a gap near the antinodes, and also directly compute the charged currents.

We start with electrons $c_{i\alpha}$ on the square lattice with dispersion

$$\mathcal{H}_c = -\sum_{i,\rho} t_\rho \left(c_{i,\alpha}^\dagger c_{i+\boldsymbol{v}_\rho,\alpha} + c_{i+\boldsymbol{v}_\rho,\alpha}^\dagger c_{i,\alpha} \right) - \mu \sum_i c_{i,\alpha}^\dagger c_{i,\alpha} + \mathcal{H}_{\text{int}} \quad (3.1)$$

As discussed above Eq. (1.2), we label *half* the links from site i by the index ρ and the vector $\boldsymbol{v}_\rho$: to avoid double-counting the vectors $\boldsymbol{v}_\rho$ do not contain any pair that add to 0. With first, second, and third neighbors, $\boldsymbol{v}_\rho$ ranges over the 6 vectors $\hat{\boldsymbol{x}}$, $\hat{\boldsymbol{y}}$, $\hat{\boldsymbol{x}} + \hat{\boldsymbol{y}}$, $-\hat{\boldsymbol{x}} + \hat{\boldsymbol{y}}$, $2\hat{\boldsymbol{x}}$, and $2\hat{\boldsymbol{y}}$.

We represent the interactions between the electrons in a 'spin-fermion' form[19] using an on-site field $\Phi^\ell(i)$, $\ell = x, y, z$, which is conjugate to the spin moment on site i:

$$\mathcal{H}_{\text{int}} = -\lambda \sum_i \Phi^\ell(i) c_{i,\alpha}^\dagger \sigma_{\alpha\beta}^\ell c_{i,\beta} + V_\Phi \tag{3.2}$$

where σ^ℓ are the Pauli matrices. We leave the effective action for Φ in V_Φ unspecified - different choices for V_Φ allow us to tune between the phases discussed below.

The key to obtaining insulators and metals with topological order (and hence a pseudogap without breaking translational symmetry) is to transform the electrons to a rotating reference frame[27,31,32,44] along the local magnetic order, using a SU(2) rotation R_i and (spinless-)fermions $\psi_{i,s}$ with $s = \pm$,

$$\begin{pmatrix} c_{i\uparrow} \\ c_{i\downarrow} \end{pmatrix} = R_i \begin{pmatrix} \psi_{i,+} \\ \psi_{i,-} \end{pmatrix}, \tag{3.3}$$

where

$$R_i^\dagger R_i = R_i R_i^\dagger = 1. \tag{3.4}$$

Note that this representation immediately introduces a SU(2) gauge invariance (distinct from the global SU(2) spin rotation)

$$\begin{pmatrix} \psi_{i,+} \\ \psi_{i,-} \end{pmatrix} \rightarrow V_i \begin{pmatrix} \psi_{i,+} \\ \psi_{i,-} \end{pmatrix} \tag{3.5}$$

$$R_i \rightarrow R_i V_i^\dagger, \tag{3.6}$$

under which the original electronic operators remain invariant, $c_{i\alpha} \rightarrow c_{i\alpha}$; here $V_i(\tau)$ is a SU(2) gauge-transformation acting on the $s = \pm$ index. So the ψ_s fermions are SU(2) gauge fundamentals, carrying the physical electromagnetic global U(1) charge, but not the SU(2) spin of the electron: they are the fermionic "chargons" of this theory, and the density of the ψ_s is the same as that of the electrons. The bosonic R fields also carry the global SU(2) spin (corresponding to left multiplication of R) but are electrically neutral: they are the bosonic "spinons". We will relate them below to the spinons, z_α, of the $\mathbb{CP}^1$ model in Eq. (2.4). A useful summary of the gauge and global symmetry quantum numbers of the various fields is in Table II.

Inserting the parameterization in Eq. (3.3) into $\mathcal{H}_{\text{int}}$, we can write Eq. (3.2) as

$$\mathcal{H}_{\text{int}} = -\lambda \sum_i H^a(i) \, \psi_{i,s}^\dagger \, \sigma_{ss'}^a \, \psi_{i,s'} + V_H \tag{3.7}$$

We have introduced here the on-site Higgs field $H^a(i)$, where $a = x, y, z$ and σ^a are the Pauli matrices. This is the spin magnetic moment transformed into the rotating reference frame, and is related to $\Phi^\ell(i)$ via

$$H^a(i) = \frac{1}{2}\Phi^\ell(i)\text{Tr}\left[\sigma^\ell R_i \, \sigma^a R_i^\dagger\right], \tag{3.8}$$

9

Field	Symbol	Statistics	$SU(2)_{\text{gauge}}$	$SU(2)_{\text{spin}}$	$U(1)_{\text{e.m.charge}}$
Electron	c	fermion	**1**	**2**	-1
Spin magnetic moment	Φ	boson	**1**	**3**	0
Chargon	ψ	fermion	**2**	**1**	-1
Spinon	R or z	boson	**$\bar{2}$**	**2**	0
Higgs	H	boson	**3**	**1**	0

TABLE II. Quantum numbers of the matter fields in the SU(2) Lattice gauge theory. The transformations under the SU(2)'s are labelled by the dimension of the SU(2) representation, while those under the electromagnetic U(1) are labeled by the U(1) charge. The spin correlations are characterized by Φ in Eq. (3.2). The Higgs field is the transform of Φ into a rotating reference frame via Eq. (3.8).

and the inverse relation

$$\Phi^\ell(i) = \frac{1}{2} H^a(i) \text{Tr} \left[\sigma^\ell R_i \, \sigma^a R_i^\dagger \right]. \tag{3.9}$$

These relations can also be written as

$$\sigma^a H^a(i) = R_i^\dagger \, \sigma^\ell \Phi^\ell(i) \, R_i. \tag{3.10}$$

The Higgs field transforms as an adjoint under the SU(2) gauge transformation, but does not carry spin or charge (see Table II)

$$H^a(i) \rightarrow \frac{1}{2} H^b(i) \text{Tr} \left[\sigma^a V_i \, \sigma^b V_i^\dagger \right], \tag{3.11}$$

or equivalently

$$\sigma^a H^a(i) \rightarrow V_i \, \sigma^b H^b(i) \, V_i^\dagger. \tag{3.12}$$

We recall in Fig. 3 an earlier mean-field phase diagram[27] obtained by condensing R or H or both. Our interest here will be primarily in phase C, which has $\mathbb{Z}_2$ topological order because the condensation of the Higgs field breaks the SU(2) invariance down to $\mathbb{Z}_2$.

We focus here on the effective Hamiltonian for the 'chargons', the ψ fermions in phase C. This is motivated by our aim of eventually computing the charge currents. To obtain the Hamiltonian, we insert the parameterization in Eq. (3.3) into the hopping terms in $\mathcal{H}_c$, and decouple the resulting quartic terms. Such an effective Hamiltonian has the form

$$\mathcal{H}_\psi = -\sum_{i,\rho} \left(w_\rho \psi_{i,s}^\dagger U_{ss'}^\rho(i) \, \psi_{i+\boldsymbol{v}_\rho,s'} + \text{H.c.} \right) - \lambda \sum_i H^a(i) \, \psi_{i,s}^\dagger \, \sigma_{ss'}^a \, \psi_{i,s'} - \mu \sum_i \psi_{i,s}^\dagger \psi_{i,s} \tag{3.13}$$

The magnitudes of the bare hoppings of the ψ fermions are determined by the real numbers w_ρ; for simplicity, we fix these hopping parameters at their bare values $w_\rho = t_\rho$. We have also included a
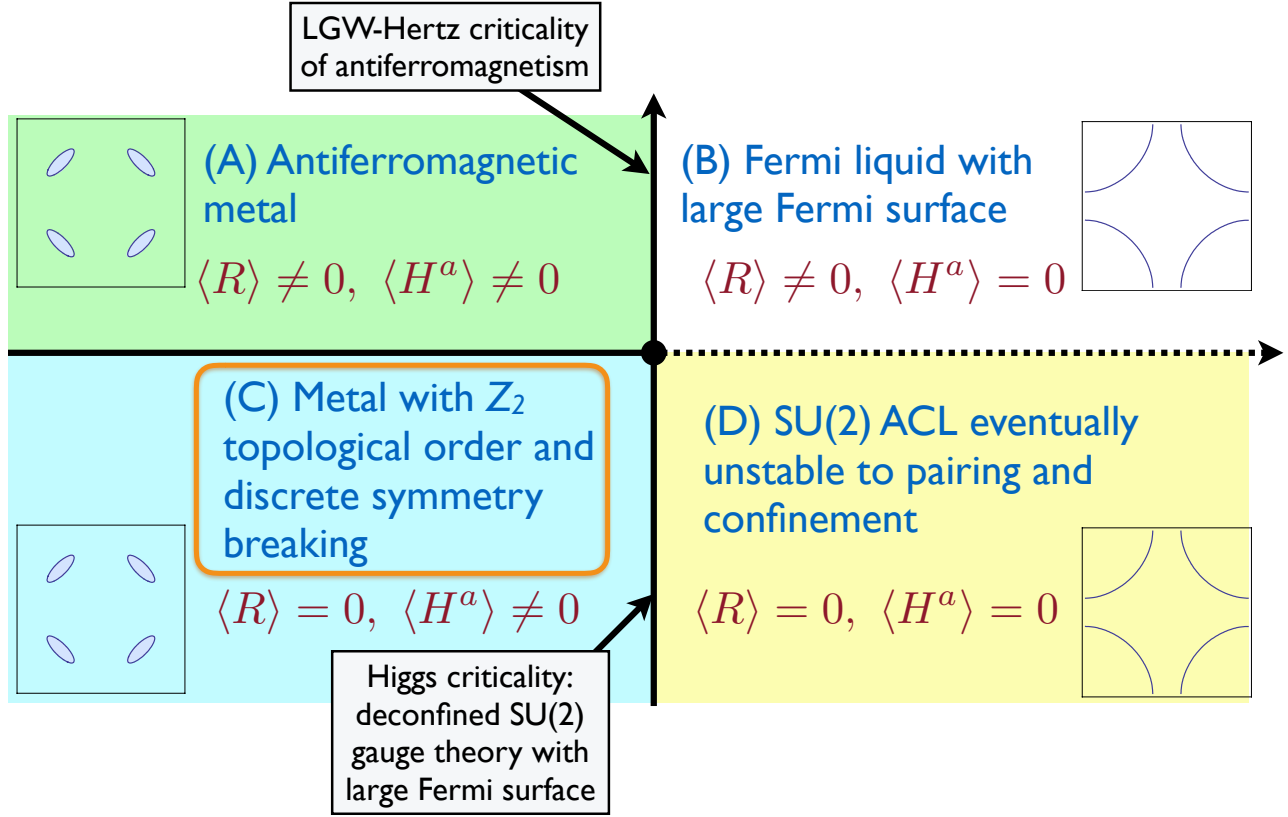
FIG. 3. Phase diagram of the SU(2) lattice gauge theory adapted from Ref. 27. The x and y axes are parameters controlling the condensates of H and R respectively. There is long-range antiferromagnetic order only in phase A. The Landau-Ginzburg-Wilson-Hertz theory[19] describing transition between the conventional phases A and B is believed to provide a suitable framework for the Fe-based superconductors.[51] The hole-doped cuprate superconductors are proposed to follow the route A-C-D-B with increasing doping. Our interest here is in the pseudogap metal phase C. The optimal doping criticality[52] is the transition from C to D, where the Higgs condensate vanishes in the presence of a large Fermi surface of fermions carrying SU(2) gauge charges. Phase D describes the overdoped regime, and is proposed to underlie the extended regime of criticality found in a magnetic field,[53] and the non-BCS superconductivity.[54]

SU(2) matrix on every link, $U^\rho(i)$, which represents the gauge connection used by the ψ fermions to hop between sites. This clearly transforms under the gauge transformation in Eq. (3.5,3.6) via

$$U^\rho(i) \to V_i U^\rho(i) V_{i+\boldsymbol{v}_\rho}^\dagger. \tag{3.14}$$

11

The previous analyses of this model[27,31,32,44] only examined the unit SU(2) matrix case $U^\rho = \mathbb{I}$. Below, we will describe other choices for U^ρ, and show that they can lead to states with spontaneous charge currents: this is the main new proposal in this paper for the SU(2) lattice gauge theory.

We will work with a translationally invariant ansatz[55] for the SU(2) gauge-charged fields, $U^\rho(i)$ and $H^a(i)$, which can be taken to be independent of i. However, to make contact with earlier formulations in which the SU(2) is broken down to a U(1) or $\mathbb{Z}_2$ gauge theory,[27,31,32] it is useful to sometimes perform a gauge transformation to a spatially-dependent ansatz. The spatially dependent form cannot be gauge transformed back to the translationally invariant form using only the U(1) or $\mathbb{Z}_2$ gauge transformations, and so the spatial dependence is not optional in the U(1) or $\mathbb{Z}_2$ gauge theories. We choose the space dependence of the SU(2) gauge fields in the following form

$$U^\rho(i) = V_i \left[\exp\left(i\theta_\rho \ell_\rho^a \sigma^a \right) \exp\left(-\frac{i}{2}(\boldsymbol{Q} \cdot \boldsymbol{v}_\rho)\sigma^z \right) \right] V_{i+\boldsymbol{v}_\rho}^\dagger$$
$$\sigma^a H^a(i) = V_i \, \sigma^b \Theta^b \, V_i^\dagger, \tag{3.15}$$

where

$$V_i = \exp\left(-\frac{i}{2}(\boldsymbol{Q} \cdot \boldsymbol{r}_i)\sigma^z \right). \tag{3.16}$$

The background gauge and Higgs fields are fully specified by the wavevector $\boldsymbol{Q}$, the 3 real numbers Θ^a, the angle θ_ρ and the unit vector ℓ_ρ^a ($\sum_{a=x,y,z}(\ell_\rho^a)^2 = 1$) on each ρ link. Note that the $\boldsymbol{r}_i$ dependence is purely in fields performing the gauge transformation so all gauge-invariant combinations will be translationally invariant. In component form, we can write Eq. (3.15) as

$$\begin{aligned} H^x(i) \pm iH^y(i) &= (\Theta^x \pm i\Theta^y)e^{\pm i\boldsymbol{Q}\cdot\boldsymbol{r}_i} \\ H^z(i) &= \Theta^z \\ U^\rho(i) &= \cos(\theta_\rho) + i\sin(\theta_\rho)\left[\ell_\rho^z \sigma^z + (\ell_\rho^x - i\ell_\rho^y)e^{-i\boldsymbol{Q}\cdot\boldsymbol{r}_i}\sigma^+ + (\ell_\rho^x + i\ell_\rho^y)e^{i\boldsymbol{Q}\cdot\boldsymbol{r}_i}\sigma^- \right] \end{aligned} \tag{3.17}$$

where $\sigma^+ = (\sigma^x + i\sigma^y)/2$.

The remaining task before us is to describe the physical properties of the phases obtained for different values of the parameters Θ^a, θ_ρ, ℓ_ρ^a which are determined by minimizing a suitable free energy. We will do this first for the previously studied phases in Section III A, and then in Section III B for the new phases obtained here. We will find that almost all ansatzes break the SU(2) gauge symmetry to a smaller gauge group: this Higgs phenomenon is accompanied by the appearance of topological order and the gapping of the fermionic spectrum to yield a pseudogap state.

Before turning to this task, we note the transformations of the ψ_i, R_i, $H^a(i)$ and $U^\rho(i)$ under symmetries in Table I. The simplest choice is to assign the transformations so that they commute with SU(2) gauge transformations. Then the transformations under spatial symmetries (T_x, T_y, I_x,

and I_y) are equal to the identity in SU(2) space, and simply given by the transformations on the spatial indices. More non-trivial are the transformations under time reversal, $\mathcal{T}$; these we assign as

$$\mathcal{T}: \psi \rightarrow -i\sigma^y\, \psi \quad , \quad R \rightarrow R \quad , \quad H \rightarrow -H \quad , \quad U \rightarrow U, \tag{3.18}$$

along with the anti-unitary complex conjugation.

We close this discussion by pausing to recall the reasoning[44,56,57] for the presence of $\mathbb{Z}_2$ topological order in the Higgs state C in which the SU(2) gauge invariance has broken down to $\mathbb{Z}_2$, and why such a state can have small Fermi pockets and a pseudogap even in the presence of translational symmetry. To break SU(2) down to $\mathbb{Z}_2$, the configuration of Higgs and link fields, Θ^a and ℓ_ρ^a, must transform under global SU(2) transformations like a SO(3) order parameter. Because $\pi_1(SO(3)) = \mathbb{Z}_2$, there are vortex line defects with single-valued Higgs and link fields. Such a defect must also correspond to a single-valued vortex configuration of the antiferromagnetic order. Now we imagine undoing the vortex configuration by choosing R such that the ψ fermions observe a locally constant background in $\mathcal{H}_\psi$. Then we will find that R is double-valued, with $R \rightarrow -R$ upon encircling a loop around the vortex. Consequently, the ψ fermions acquire a Berry phase of π around the vortex, and the ψ fermions and vortex excitations (the 'visons'[58]) are relative semions. These vortices will be suppressed in the Higgs-condensed ground state, and in such a ground state we can globally transform to a rotating reference frame in which the ψ fermions are described by $\mathcal{H}_\psi$. The $\boldsymbol{Q}$ dependent configuration of Higgs and link fields in Eq. (3.17) can then reconstruct the ψ Fermi surface into pockets.

A.   Previously studied phases

1.   Insulators with Néel or VBS order

These are obtained from the saddle point with $\boldsymbol{Q} = (\pi, \pi)$ and $\Theta^a = (\Theta, 0, 0)$, while all the $\theta_\rho = 0$ so that $U^\rho = \mathbb{I}$. The Higgs field has two sublattice order polarized the x direction with $H^a(i) = \eta_i(\Theta, 0, 0)$ where $\eta_i = \pm 1$ on the two sublattices.

The dispersion of the ψ fermions is the same as that of electrons in the presence of Néel order, and we obtain the needed fermionic gap in the anti-nodal regions of the Brillouin zone. Note however that Eq. (3.9) implies that the appearance of physical Néel order requires the condensation of R. We assume Θ is large, and choose the chemical potential to lie within the band gap which has magnitude $|\Theta|$. Consequently, the ψ fermions form a band insulator, and the charge gap is of order $|\Theta|$ which we assume is of order the U of the underlying Hubbard model.

We now argue that fluctuations about this 'band insulator' saddle point are described by the $\mathbb{CP}^1$ model of Eq. (2.4). A key observation is that presence of the Higgs condensate $H^a(i) = \eta_i(\Theta, 0, 0)$

breaks the SU(2) gauge invariance down to U(1). Such a Higgs condensate is invariant under residual U(1) gauge transformations about the x axis. So we parameterize the the fluctuations of the link fields by

$$U^\rho = \exp\left(i\sigma^x \boldsymbol{a} \cdot v_{\boldsymbol{\rho}}\right); \tag{3.19}$$

then $\boldsymbol{a}$ transforms like the spatial component of a U(1) gauge field under the residual gauge transformation. To obtain the spinons z_α in Eq. (2.4), we need to parameterize R in terms z_α so that Eq. (3.6) implies that z_α have unit gauge charge under the gauge transformation $V = \exp(i\sigma^x\zeta)$, where ζ generates the gauge transformation. This is obtained from

$$R = \frac{1}{\sqrt{2}} \begin{pmatrix} z_\uparrow + z_\downarrow^* & -z_\downarrow^* + z_\uparrow \\ z_\downarrow - z_\uparrow^* & z_\uparrow^* + z_\downarrow \end{pmatrix}, \tag{3.20}$$

under which $z_\alpha \to z_\alpha e^{-i\zeta}$.

We note here a subtlety in identifying the z_α and $\boldsymbol{a}$ above with the fields of the $\mathbb{CP}^1$ model of Eq. (2.4): the symmetry assignments discussed near Eq. (3.18) for the SU(2) gauge theory do not map under Eq. (3.19) to the symmetry assignments in Table I and Ref. 59. The difference is present for transformations T_x, T_y and $\mathcal{T}$, under which the Higgs field $\Theta \to -\Theta$ in the SU(2) formulation for $\boldsymbol{Q} = (\pi, \pi)$. In the $\mathbb{CP}^1$ formulation, it is implicitly assumed that the Higgs field is invariant under all transformations. To remedy this, we need to combine the SU(2) gauge transformation $V = \exp(-i(\pi/2)\sigma^z)$ with the operations of T_x, T_y, and $\mathcal{T}$ in the SU(2) gauge theory.

Beyond the fluctuations described by the $\mathbb{CP}^1$ model, we have to consider the non-perturbative role of monopoles in the U(1) gauge field.[36,37] In the earlier works, the spin liquid was described using Schwinger bosons with a unit boson density per site. In the presence of monopoles, this background density of bosons contributed a net Berry phase.[37] In the present formulation, we have a background of a filled band of the ψ fermions. The monopole Berry phase computation of Ref. 37 (Section III.A) carries over with little change to the fermion case, and we obtain the same monopole Berry phases.

The remaining analysis of the $\mathbb{CP}^1$ model augmented with monopole Berry phases is as before.[36–39] The phase with $\langle z_\alpha \rangle \neq 0$ has Néel order, while the strong coupling phase $\langle z_\alpha \rangle = 0$ is initially a U(1) spin liquid which eventually confines at the longest scales to a VBS; the transition between these phase is described by the critical $\mathbb{CP}^1$ model.

2. Insulators with spiral spin order or $\mathbb{Z}_2$ topological order

The saddle point is similar to that in Section III A 1, except that $\boldsymbol{Q}$ is incommensurate. So we have $\Theta^a = (\Theta, 0, 0)$, while all the $\theta_\rho = 0$ so that $U^\rho = \mathbb{I}$. Eq. (3.15) implies that the spatial

dependence of the Higgs field is specified by

$$H^a(i) = \Theta(\cos(\boldsymbol{Q} \cdot \boldsymbol{r}_i), \sin(\boldsymbol{Q} \cdot \boldsymbol{r}_i), 0). \tag{3.21}$$

For generic $\boldsymbol{Q}$, there is no residual U(1) gauge invariance left by such a condensate. Instead, the only residual gauge invariance is $\mathbb{Z}_2$, associated with the choice $V_i = \pm 1$. Consequently, the spin liquid described by this Higgs condensate has $\mathbb{Z}_2$ topological order. Again, to obtain an insulator we assume that the chemical potential is within the gap of the ψ bands.

The phases obtain by Eq. (3.21) are precisely those described in Refs. 28, 29, and 60, and the earlier analyses can be applied directly here. The phase with R condensed has spiral spin order, while the phase with R gapped is a $\mathbb{Z}_2$ spin liquid.

3. Metals with topological order

A key advantage of the present SU(2) gauge theory formulation is that the results obtained in Sections III A 1 and III A 2 are immediately generalized from insulators to metals. One only has to change the chemical potential μ so that one of the ψ bands is partially occupied, and we obtain a Fermi surface of ψ chargons.

For the $U(1)$ gauge theory in Section III A 1, the ψ Fermi surface can suppress the monopoles, and the U(1) topological order survives in an 'algebraic charge liquid' (ACL).[47] The $\mathbb{Z}_2$ topological order was already stable in the insulator in Section III A 2, and it continues to survive in the presence of the ψ Fermi surface.

It is also possible that the ACL becomes a 'fractionalized Fermi liquid' (FL*).[21–23] This appears when the ψ fermions bind with the R spinons to form 'small' Fermi surfaces of electron-like quasiparticles[24,25,47,49] while retaining the topological order.

B. States with SU(2) gauge fields on links

We turn to our new results on the SU(2) lattice gauge theory. We will examine saddle points with non-zero Higgs condensate $\langle H \rangle \neq 0$ (as above) and also a non-trivial background gauge flux $U^\rho \neq \mathbb{I}$. We will find that such saddle points can break time-reversal and inversion symmetries in gauge-invariant observables, and that is sufficient to induce charge currents. Ising-nematic order can also be present, as found previously, but it can also co-exist with spontaneous charge currents. This subsection will report results in the gauge $\boldsymbol{Q} = 0$. Recall that the value of $\boldsymbol{Q}$ is merely a gauge choice in the full SU(2) gauge theory (but not in U(1) or $\mathbb{Z}_2$ gauge theory formulations). In this gauge, the Higgs field is i independent with $H^a(i) = \Theta^a$.

Formally, we should integrate out the fermions in $\mathcal{H}_\psi$ in Eq. (3.13), and then minimize the resulting action functional for the Higgs and gauge fields. However, this is computationally demanding, and the structure assumed in $\mathcal{H}_\psi$ is phenomenological anyway. So we will be satisfied by minimizing a phenomenological gauge-invariant functional of the Higgs and gauge fields, consisting of short-range terms that can be constructed out of a single plaquette. In metallic states, the fermion determinant can also induce longer-range terms with a power-law decay, but we will not include those here: in our simple treatment, we assume that the dominant energy arises from the short-range terms.

The effective potential also has terms contributing to a Higgs potential V_H which arise from V_Φ in Eq. (3.2) via Eq. (3.9). As we will not specify V_H, we assume that this potential has already been minimized to yield the values of Θ^a. So we will only consider the remaining free energy, $\mathcal{F}$, which is a function only of the U^ρ.

The following gauge-invariant link variables are useful ingredients in constructing the free energy

$$\mathcal{L}^\rho = \Theta^a \Theta^b \operatorname{Tr}(\sigma^a U^\rho \sigma^b U^{\rho\dagger}); \tag{3.22}$$

These link variables are even under the time-reversal operation described in Eq. (3.18). In terms of these link variables, we can define the nematic order parameters in Eq. (1.5) by

$$\mathcal{N}_1 = \mathcal{L}^1 - \mathcal{L}^2 \quad , \quad \mathcal{N}_2 = \mathcal{L}^3 - \mathcal{L}^4. \tag{3.23}$$

In writing the free energy, it is useful to change notation and write the link variables via

$$U^\rho(i) \to U_{ij} \quad , \text{with } \boldsymbol{r}_j = \boldsymbol{r}_i + \boldsymbol{v}_\rho. \tag{3.24}$$

We minimized the free energy

$$\begin{aligned}
\mathcal{F} = {}& K_1 \left(\mathcal{L}^1 + \mathcal{L}^2 \right) + K_8 (\mathcal{L}^1 - \mathcal{L}^2)^2 + K_9 \left(\mathcal{L}^3 - \mathcal{L}^4 \right)^2 \\
& + \sum_{\substack{k \\ j\triangle i}} \Big[K_3 \operatorname{Tr} \left(U_{ij} U_{jk} U_{ki} \right) + K_4 \left[\operatorname{Tr} \left(U_{ij} U_{jk} U_{ki} \right) \right]^2 + K_5 \operatorname{Tr} \left(U_{ij} U_{jk} \sigma^a U_{ki} \sigma^b \right) \Theta^a \Theta^b \\
& - K_6 \operatorname{Tr} \left(U_{ij} \sigma^a U_{jk} U_{ki} \sigma^b \right) \Theta^a \Theta^b \Big] + \sum_{\substack{k \quad \ell \\ j\square i}} K_7 \operatorname{Tr} \left(U_{ij} U_{jk} U_{k\ell} U_{\ell i} \right). \tag{3.25}
\end{aligned}$$

In the above expressions we assume that all terms obtained from the pictured symbols by square lattice symmetry operations have been summed over. This free energy depends upon 9 parameters K_{1-9}, and a priori they are free to take arbitrary values. We used the residual SU(2) gauge degree for freedom to set $\Theta^a = (\Theta, 0, 0)$, and then with 4 possible values of the link variable ρ, the free depends upon 12 real numbers which determine the U^ρ.

16

We characterized the free energy minima by their values of the nematic order parameters $\mathcal{N}_1$ and $\mathcal{N}_2$. We also need gauge-invariant observables which are odd under time-reversal; for this we evaluated the combinations defined on right triangles, ijk:

$$\mathcal{P}_{ijk} = i \, \mathrm{Tr} \left(\sigma^a U_{ij} U_{jk} U_{ki} \right) H^a(i). \tag{3.26}$$

The spatial patterns of the $\mathcal{P}_{ijk}$, along with the values of $\mathrm{Tr} \left(U_{ij} U_{jk} U_{ki} \right)$, yield much information on the nature of time-reversal and inversion symmetry breaking. Note that the $\mathcal{P}_{ijk}$ are non-zero only if the Higgs field is non-zero—this is a consequence of the transformation in Eq. (3.18). So time-reversal symmetry can only be broken in states in which the SU(2) gauge invariance is also broken.

Another important characterization of the states is provided by the values of the physical charge current. We used the values of the link variables obtained by the minimization of $\mathcal{F}$, and inserted them into the Hamiltonian $\mathcal{H}_\psi$ in Eq. (3.13). We then determined the current on each link by evaluating the expectation value of the current operator

$$\boldsymbol{J}_\rho(i) = -i\boldsymbol{v}_\rho \left(w_\rho \psi_{i,s}^\dagger \, U_{ss'}^\rho(i) \, \psi_{i+\boldsymbol{v}_\rho,s'} - \mathrm{H.c.} \right) \tag{3.27}$$

in the fermion state specified by the Hamiltonian $\mathcal{H}_\psi$ at a low temperature. As shown in Appendix A, for the background field configurations in Eq. (3.17), $\langle \boldsymbol{J}_\rho(i) \rangle$ turns out to be independent of i for general values of the variational parameters Θ^a, θ_ρ, ℓ_ρ^a and $\boldsymbol{Q}$ in the Hamiltonian. This is as expected from our arguments that Eq. (3.17) implies that all gauge-invariant observables should be translationally invariant. Moreover, we find that the value of $\langle \boldsymbol{J}_\rho \rangle$ always obeys Bloch's theorem in Eq. (1.2); this is true in our numerics, and a general proof is in Appendix A.

It is also useful to examine local gauge-invariant operators which have the same symmetry signatures as the physical current $\boldsymbol{J}_\rho$. Such operators will be realizations of the operator $\boldsymbol{O}$ characterizing states with broken inversion and time-reversal symmetry. We obtained expressions using the symmetry transformations described near Eq. (3.18), and one set of operators is presented in Fig. 4. A derivation based upon a large $|H^a(i)|$ expansion is presented in Appendix C, along with other sets of possible operators. For the translationally invariant solution and $\boldsymbol{Q} = 0$ gauge being considered here, Fig. 4 yields these expressions for the order parameters O_ρ along the directions $\boldsymbol{v}_\rho$:

$$O_1 = i \, \mathrm{Tr} \left(\sigma^a U^1 U^{2\dagger} U^4 \right) \Theta^a - i \, \mathrm{Tr} \left(\sigma^a U^{1\dagger} U^{2\dagger} U^3 \right) \Theta^a + i \, \mathrm{Tr} \left(\sigma^a U^1 U^2 U^{3\dagger} \right) \Theta^a - i \, \mathrm{Tr} \left(\sigma^a U^{1\dagger} U^2 U^{4\dagger} \right) \Theta^a$$

$$O_2 = i \, \mathrm{Tr} \left(\sigma^a U^2 U^1 U^{3\dagger} \right) \Theta^a - i \, \mathrm{Tr} \left(\sigma^a U^{2\dagger} U^1 U^4 \right) \Theta^a + i \, \mathrm{Tr} \left(\sigma^a U^2 U^{1\dagger} U^{4\dagger} \right) \Theta^a - i \, \mathrm{Tr} \left(\sigma^a U^{2\dagger} U^{1\dagger} U^3 \right) \Theta^a$$

$$O_3 = i \, \mathrm{Tr} \left(\sigma^a U^2 U^1 U^{3\dagger} \right) \Theta^a - i \, \mathrm{Tr} \left(\sigma^a U^{1\dagger} U^{2\dagger} U^3 \right) \Theta^a + i \, \mathrm{Tr} \left(\sigma^a U^1 U^2 U^{3\dagger} \right) \Theta^a - i \, \mathrm{Tr} \left(\sigma^a U^{2\dagger} U^{1\dagger} U^3 \right) \Theta^a$$

$$O_4 = i \, \mathrm{Tr} \left(\sigma^a U^2 U^{1\dagger} U^{4\dagger} \right) \Theta^a - i \, \mathrm{Tr} \left(\sigma^a U^1 U^{2\dagger} U^4 \right) \Theta^a + i \, \mathrm{Tr} \left(\sigma^a U^{1\dagger} U^2 U^{4\dagger} \right) \Theta^a - i \, \mathrm{Tr} \left(\sigma^a U^{2\dagger} U^1 U^4 \right) \Theta^a$$

$$\tag{3.28}$$
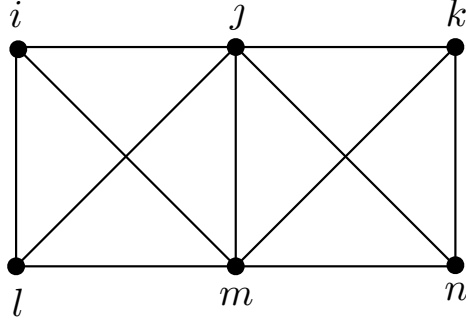
$$O_{mj} = i\,\mathrm{Tr}\left(\sigma^a U_{mj} U_{jk} U_{km}\right) H^a(m)$$
$$- i\,\mathrm{Tr}\left(\sigma^a U_{jm} U_{mn} U_{nj}\right) H^a(j)$$
$$+ i\,\mathrm{Tr}\left(\sigma^a U_{mj} U_{ji} U_{im}\right) H^a(m)$$
$$- i\,\mathrm{Tr}\left(\sigma^a U_{jm} U_{ml} U_{lj}\right) H^a(j)$$

$$O_{mk} = i\,\mathrm{Tr}\left(\sigma^a U_{mj} U_{jk} U_{km}\right) H^a(m)$$
$$- i\,\mathrm{Tr}\left(\sigma^a U_{kj} U_{jm} U_{mk}\right) H^a(k)$$
$$+ i\,\mathrm{Tr}\left(\sigma^a U_{mn} U_{nk} U_{km}\right) H^a(m)$$
$$- i\,\mathrm{Tr}\left(\sigma^a U_{kn} U_{nm} U_{mk}\right) H^a(k)$$

FIG. 4. Expressions for the time and inversion symmetry breaking order parameter $\boldsymbol{O}$ in terms of the variables of the SU(2) gauge theory. We use the same notation as in Eq. (3.24) for the link values of $U^\rho(i)$ and $\boldsymbol{O}$ with $O_{ij} = \boldsymbol{O} \cdot \boldsymbol{v}_\rho$ when $\boldsymbol{r}_j = \boldsymbol{r}_i + \boldsymbol{v}_\rho$.

These will be connected to $\boldsymbol{J}_\rho$ via an expression like Eq. (1.3). Note that the O_ρ can only be non-zero when the Higgs condensate is non-zero, because only the Higgs field is odd under time-reversal in Eq. (3.18). An explicit demonstration that a non-zero charge current requires a non-zero Higgs field is in Appendix B.

Turning to the minimization of $\mathcal{F}$ in Eq. (3.25), we did not perform an exhaustive search of different classes of states over the 9 parameters, K_{1-9} in $\mathcal{F}$. Rather we explored a few values to yield representative minima, and will describe a few of the typical states in the subsections below. All of the minimization was performed with the Higgs field oriented along the x direction, $\Theta^a = (\Theta, 0, 0)$.

1. Symmetric state

This state preserves all square lattice symmetries and time reversal. We obtained such a minimum at $K_1 = 1$, $K_2 = -1$, $K_3 = 2$, $K_4 = 2$, $K_5 = 2$, $K_6 = 2$, $K_7 = 0.1$, $K_8 = 0$, $K_9 = 0$. In the

18

$\boldsymbol{Q} = 0$ gauge, the link fields take the values:

$$U^1 = i\sin(\theta)\,\sigma^x - i\cos(\theta)\,\sigma^y$$
$$U^2 = i\sin(\theta)\,\sigma^x + i\cos(\theta)\,\sigma^y$$
$$U^3 = -1$$
$$U^4 = 1, \tag{3.29}$$

where $\theta = 0.344\pi$. All the O_ρ, $\mathcal{N}_1$ and $\mathcal{N}_2$ order parameters, and the currents $\boldsymbol{J}_\rho$, vanish in this state. The SU(2) gauge invariance is broken down to $\mathbb{Z}_2$ because the U^ρ and Θ^a have no common orientation, and so this state has $\mathbb{Z}_2$ topological order.

2. Ising-nematic order

This state preserves time reversal and inversion, but breaks a square lattice rotation symmetry. We obtained such a minimum at $K_1 = 0.5$, $K_2 = 0.5$, $K_3 = -1$, $K_4 = 0.25$, $K_5 = 0$, $K_6 = 0$, $K_7 = 0$, $K_8 = 0$, $K_9 = 5$. In the $\boldsymbol{Q} = 0$ gauge the link fields take the values:

$$U^1 = -i\,\sigma^z$$
$$U^2 = \cos(\theta_1) + i\sin(\theta_1)\,\sigma^z$$
$$U^3 = \cos(\theta_2) + i\sin(\theta_2)\,\sigma^z$$
$$U^4 = -\cos(\theta_2) - i\sin(\theta_2)\,\sigma^z \tag{3.30}$$

where $\theta_1 = 0.672\pi$ and $\theta_2 = 0.427\pi$. All the O_ρ, and the currents $\boldsymbol{J}_\rho$, vanish in this state. However the nematic order $\mathcal{N}_1 \neq 0$, while $\mathcal{N}_2 = 0$. Note that the U^ρ are oriented along a common z direction, while the Higgs field Θ^a is oriented along the distinct x direction. So SU(2) gauge invariance is broken down $\mathbb{Z}_2$, and $\mathbb{Z}_2$ topological order is present. In the insulator, this state has the same properties as the "(π, q) SRO" state of Refs. 28 and 29.

3. State with broken time-reversal

Now we present a state which breaks time-reversal but *not* inversion. So this state has no spontaneous currents, and $O^\rho = 0$ and $\boldsymbol{J}^\rho = 0$. Nevertheless, time reversal is broken as signaled by the non-zero values of some of the $\mathcal{P}_{ijk}$. Roughly speaking, such a state has spontaneous currents along different directions in the gauge group, but the net electromagnetic current vanishes. We obtained such a minimum at $K_1 = 0.5$, $K_2 = 0.5$, $K_3 = 1$, $K_4 = 0.667$, $K_5 = 0$, $K_6 = 0$, $K_7 = 1$,

$K_8 = 5$, $K_9 = 5$. In the $\boldsymbol{Q} = 0$ gauge the link fields take the values:

$$U^1 = -\cos(\theta_1) - i\sin(\theta_1)\,\sigma^z$$
$$U^2 = \cos(\theta_1) + i\sin(\theta_1)\,\sigma^y$$
$$U^3 = \cos(\theta_2) + i\sin(\theta_2)\,(\sigma^y + \sigma^z)/\sqrt{2}$$
$$U^4 = -\cos(\theta_2) + i\sin(\theta_2)\,(\sigma^y - \sigma^z)/\sqrt{2}, \tag{3.31}$$

where $\theta_1 = 0.446\pi$ and $\theta_2 = 0.497\pi$. Again, SU(2) gauge invariance is broken down $\mathbb{Z}_2$, and $\mathbb{Z}_2$ topological order is present.

4. States with spontaneous charge currents.

Finally, we turn to a description of the states presented in Fig. 2.

First, we present a state with the symmetry of Fig. 2a. Such a state was obtained for $K_1 = 0.5$, $K_2 = 0.5$, $K_3 = -1$, $K_4 = 0.25$, $K_5 = 0$, $K_6 = 0$, $K_7 = 0$, $K_8 = 2$, $K_9 = 5$. In the $\boldsymbol{Q} = 0$ gauge the link fields take the values

$$U^1 = \cos(\theta_1) + i\sin(\theta_1)\,(\cos(\phi_1)\sigma^x + \sin(\phi_1)\sigma^z)$$
$$U^2 = i\,(\cos(\phi_2)\sigma^x + \sin(\phi_2)\sigma^z)$$
$$U^3 = -\cos(\theta_2) + i\sin(\theta_2)\,(\cos(\phi_1)\sigma^x + \sin(\phi_1)\sigma^z)$$
$$U^4 = \cos(\theta_2) + i\sin(\theta_2)\,(\cos(\phi_1)\sigma^x + \sin(\phi_1)\sigma^z) \tag{3.32}$$

where $\theta_1 = 0.410\pi$, $\phi_1 = 0.5063\pi$, $\phi_2 = 0.558\pi$, $\theta_2 = 0.387\pi$. This state has the O^ρ and $\boldsymbol{J}^\rho$ non-zero, along with a non-zero Ising-nematic order $\mathcal{N}_1 \neq 0$, but $\mathcal{N}_2 = 0$. So it has the full generic symmetry structure of Fig. 2a. The gauge field configuration shows that SU(2) is broken down to $\mathbb{Z}_2$, and so $\mathbb{Z}_2$ topological order is present. States in this class were the most common in our search over the parameters K_{1-9} among those that broke time-reversal symmetry.

Among states with a residual U(1) gauge invariance, we found global minima with the symmetry of Fig. 2a only when we restricted the search to states in which the Higgs and link fields were collinear in the gauge SU(2) space. We can parameterize the fluctuations about such a saddle point by multiplying the U^ρ by the factor in Eq. (3.19), and then we obtain a theory of a gapless U(1) photon a_μ. Because of the presence of the breaking of inversion and time-reversal symmetries, this action will take the form in Eq. (2.8), including the term proportional to $\boldsymbol{\Gamma}$. As in Section III A 1, we have to consider the non-perturbative effects of monopoles: such a state can be stable against monopole proliferation only in the presence of gauge-charged Fermi surfaces.

Next, we present a state with the symmetry of Fig. 2b. Such a state was obtained for $K_1 = 0.5$, $K_2 = 0.5$, $K_3 = 1$, $K_4 = 0.667$, $K_5 = 0$, $K_6 = 0$, $K_7 = 0$, $K_8 = 5$, $K_9 = -1$. In the $\boldsymbol{Q} = 0$ gauge

the link fields take the values

$$U^1 = -\cos(\theta_1) - i\sin(\theta_1)\,\sigma^z$$
$$U^2 = \cos(\theta_1) + i\sin(\theta_1)\,\sigma^z$$
$$U^3 = \cos(\theta_2) + i\sin(\theta_2)\,\sigma^z$$
$$U^4 = \cos(\theta_3) - i\sin(\theta_3)\,\sigma^x \tag{3.33}$$

where $\theta_1 = 0.451\pi$, $\theta_2 = 0.503\pi$, $\theta_3 = 0.379\pi$. The order parameters O^ρ and the currents $\boldsymbol{J}^\rho$ are non-zero, and are consistent with the pattern in Fig. 2a. There is also a non-zero Ising-nematic order $\mathcal{N}_2 \neq 0$, but $\mathcal{N}_1 = 0$. The non-collinear alignment of the gauge and Higgs fields indicates the presence of $\mathbb{Z}_2$ topological order.

IV. CONCLUSIONS

We have presented computations showing that emergent background gauge connections, and associated Berry phases, arising from the local antiferromagnetic spin correlations can induce spontaneous charge currents, while preserving translational symmetry. The main requirement on the gauge theory is that *gauge-invariant* observables break time-reversal and inversion, but preserve translation. At the same time, the topological order associated with the emergent gauge fields can account for the anti-nodal gap in the charged fermionic excitations.

The specific model we used for a stable pseudogap metal had $\mathbb{Z}_2$ topological order. We employed a SU(2) lattice gauge theory with a Higgs field to realize such a phase. Going beyond earlier work on this theory, we allowed the SU(2) gauge fields on the links to acquire non-trivial values in the saddle point of the Higgs phase. These link fields had two important consequences. First, it became possible to obtain $\mathbb{Z}_2$ topological order even under conditions in which the proximate magnetically ordered phase had collinear spin correlations at (π, π); earlier realizations[27–29,31,32] required non-collinear spiral spin correlations. Second, the gauge-invariant combinations of the SU(2) gauge fluxes and the Higgs field could break time-reversal and inversion symmetries without breaking translational symmetry. This allowed the appearance of spontaneous charge currents and Ising-nematic order in the Higgs phase. Linking the discrete broken symmetries to the presence of the Higgs condensate also explains why the broken symmetries do not survive in the confining phases at large doping.

An attractive features of our results is that the charge currents, and the anti-nodal gap, continue largely unmodified across transitions to states with long-range antiferromagnetic order, but without topological order. This is consistent with recent experiments[11,13] on $\mathrm{Sr_2Ir_{1-x}Rh_xO_4}$ showing co-existence of Néel order and inversion and time reversal breaking over a certain range of doping and temperature.

The possible patterns of symmetry breaking in the translationally-invariant states with broken time-reversal and inversion (but not their product) are illustrated in Fig. 2. Both states also break a lattice rotation symmetry, and so they also have Ising-nematic order. The state in Fig. 2b has the same pattern of symmetry breaking as states considered earlier.[16,42,43] However, the state in Fig. 2a does not appear to have been described previously in the literature. The Fig. 2a state has the attractive feature that its Ising-nematic order is precisely that observed in other experiments.[1,3,6,8] The onset of Ising-nematic order and time-reversal and inversion symmetry breaking could happen at the same or distinct temperatures, as we also found states in Section III B 2 with Ising-nematic order but no charge currents. However, if a particular symmetry is broken in the pseudogap phase (phase C in Fig. 3), it must be restored when the Higgs condensate vanishes in the over-doped regime (phases D and B in Fig. 3).

The existing experiments[11,13] do not contain the polarization analysis needed to distinguish between the states in Fig. 2a and b, and we hope such experiments will be undertaken.

We placed our results in the context of a global phase diagram for antiferromagnetism and superconductivity in two dimensions in Fig. 3. In particular, we noted that this phase diagram[27,31,32] is in accord with experiments exploring the hole-doped cuprates over a range of carrier density. Badoux et $al.$[52] observe pseudogap metal at low T and large doping, without any charge density wave order: this is a candidate for our phase C. We note recent theoretical works[61,62] which studied electrical and thermal transport across the phase transition C $\to$ D in Fig. 3, and found results in good accord with observations.[52,63–65] Cooper et $al.$[53] observe an extended overdoped regime of linear-in-T resistivity when the superconductivity is suppressed by a magnetic field: our phase D could be such a critical phase. And Božović et $al.$[54] see strong deviations from BCS theory in the doping and temperature dependence of the superfluid stiffness in the overdoped regime: this could also be described by phase D.

Appendix A: Momentum space

This appendix presents a few expressions from Section III in momentum space. These expressions were used for our numerical computation.

The momentum space form of the electron dispersion in Eq. (3.1) is

$$\mathcal{H}_c = -2 \sum_{\boldsymbol{k},\rho} t_\rho \cos(\boldsymbol{k} \cdot \boldsymbol{v}_\rho) c_{\boldsymbol{k},\alpha}^\dagger c_{\boldsymbol{k},\alpha} - \mu \sum_{\boldsymbol{k}} c_{\boldsymbol{k},\alpha}^\dagger c_{\boldsymbol{k},\alpha} + \mathcal{H}_{\text{int}}. \tag{A1}$$

The Hamiltonian for the ψ fermions is obtained from Eqs. (3.13) and (3.17) (we have set $\lambda = -1$)):

$$\mathcal{H}_\psi = \sum_{\boldsymbol{k}} \psi_{\boldsymbol{k},+}^\dagger \left(-\mu + \Theta^z - 2 \sum_\rho w_\rho \Big[\cos(\theta_\rho)\cos(\boldsymbol{k}\cdot\boldsymbol{v}_\rho) - \ell_\rho^z \sin(\theta_\rho)\sin(\boldsymbol{k}\cdot\boldsymbol{v}_\rho) \Big] \right) \psi_{\boldsymbol{k},+}$$

$$+ \sum_{\boldsymbol{k}} \psi_{\boldsymbol{k}+\boldsymbol{Q},-}^\dagger \left(-\mu - \Theta^z - 2 \sum_\rho w_\rho \Big[\cos(\theta_\rho)\cos((\boldsymbol{k}+\boldsymbol{Q})\cdot\boldsymbol{v}_\rho) + \ell_\rho^z \sin(\theta_\rho)\sin((\boldsymbol{k}+\boldsymbol{Q})\cdot\boldsymbol{v}_\rho) \Big] \right) \psi_{\boldsymbol{k}+\boldsymbol{Q},-}$$

$$+ \sum_{\boldsymbol{k}} \psi_{\boldsymbol{k},+}^\dagger \psi_{\boldsymbol{k}+\boldsymbol{Q},-} \left(\Theta^x - i\Theta^y + \sum_\rho w_\rho \sin(\theta_\rho)(\ell_\rho^x - i\ell_\rho^y)\Big[-ie^{i(\boldsymbol{k}+\boldsymbol{Q})\cdot\boldsymbol{v}_\rho} + ie^{-i\boldsymbol{k}\cdot\boldsymbol{v}_\rho} \Big] \right) + \text{H.c.}. \tag{A2}$$

The average kinetic energy and current on each bond can be evaluated from

$$-\left\langle w_\rho \psi_i^\dagger \, U^\rho(i) \, \psi_{i+\boldsymbol{v}_\rho} \right\rangle = -w_\rho \Big[\cos(\theta_\rho) + i\ell_\rho^z \sin(\theta_\rho) \Big] \sum_{\boldsymbol{k}} e^{i\boldsymbol{k}\cdot\boldsymbol{v}_\rho} \left\langle \psi_{\boldsymbol{k},+}^\dagger \psi_{\boldsymbol{k},+} \right\rangle$$

$$-w_\rho \Big[\cos(\theta_\rho) - i\ell_\rho^z \sin(\theta_\rho) \Big] \sum_{\boldsymbol{k}} e^{i(\boldsymbol{k}+\boldsymbol{Q})\cdot\boldsymbol{v}_\rho} \left\langle \psi_{\boldsymbol{k}+\boldsymbol{Q},-}^\dagger \psi_{\boldsymbol{k}+\boldsymbol{Q},-} \right\rangle$$

$$-iw_\rho \sin(\theta_\rho)(\ell_\rho^x - i\ell_\rho^y) \sum_{\boldsymbol{k}} e^{i(\boldsymbol{k}+\boldsymbol{Q})\cdot\boldsymbol{v}_\rho} \left\langle \psi_{\boldsymbol{k},+}^\dagger \psi_{\boldsymbol{k}+\boldsymbol{Q},-} \right\rangle$$

$$-iw_\rho \sin(\theta_\rho)(\ell_\rho^x + i\ell_\rho^y) \sum_{\boldsymbol{k}} e^{i\boldsymbol{k}\cdot\boldsymbol{v}_\rho} \left\langle \psi_{\boldsymbol{k}+\boldsymbol{Q},-}^\dagger \psi_{\boldsymbol{k},+} \right\rangle. \tag{A3}$$

Note that the result is explicitly independent of the site i. The kinetic energy is twice the real part of the result, while the current, $\boldsymbol{J}_\rho$ in Eq. (3.27), is $-\boldsymbol{v}_\rho$ times the imaginary part.

From the expression in momentum space, it is straightforward to see that the value of $\langle \boldsymbol{J}_\rho \rangle$ always obeys Bloch's theorem. The Hamiltonian H_ψ can be re-written in momentum space in terms of a 2-component spinor $\chi_{\boldsymbol{k}}$ as follows:

$$H_\psi = \sum_{\boldsymbol{k}} \chi_{\boldsymbol{k}}^\dagger \, h_{\boldsymbol{k}} \, \chi_{\boldsymbol{k}}, \text{ where } \chi_{\boldsymbol{k}} = \begin{pmatrix} \psi_{\boldsymbol{k},+} \\ \psi_{\boldsymbol{k}+\boldsymbol{Q},-} \end{pmatrix}. \tag{A4}$$

The minimal coupling to an external electromagnetic gauge field $\boldsymbol{A}$ corresponds to a transformation $\boldsymbol{k} \to \boldsymbol{k} - \boldsymbol{A}$ in the momentum space Hamiltonian $h_{\boldsymbol{k}}$. The operator for the net current $\mathbf{J}$ in any

given direction is the negative of the derivative with respect to $\boldsymbol{A}$ at $\boldsymbol{A} = 0$, which can be recast as a derivative with respect to $\boldsymbol{k}$:

$$\sum_\rho \langle \mathbf{J}_\rho \rangle = \sum_\rho \int \frac{d^2k}{(2\pi)^2} \langle \mathbf{J}_\rho(\boldsymbol{k}) \rangle = \int \frac{d^2k}{(2\pi)^2} \langle \chi_{\boldsymbol{k}}^\dagger \frac{\partial h_{\boldsymbol{k}}}{\partial \boldsymbol{k}} \chi_{\boldsymbol{k}} \rangle = \int \frac{d^2k}{(2\pi)^2} \frac{\partial}{\partial \boldsymbol{k}} \langle \chi_{\boldsymbol{k}}^\dagger h_{\boldsymbol{k}} \chi_{\boldsymbol{k}} \rangle = 0, \quad \text{(A5)}$$

where the last step uses the Feynman-Hellman theorem and periodicity in the Brillouin zone.

Appendix B: Relation between loop currents and Higgs condensate

We show that a non-zero current necessarily requires a Higgs condensate. To do so, we need an operator which reverses the current, and is a symmetry of the Hamiltonian only if the Higgs condensate is absent. Consider the following anti-unitary operator T that leaves the Higgs field unchanged:

$$T \psi_{s,\boldsymbol{k}} T^{-1} = (-i\tau^y)_{s,s'} \psi_{s',-\boldsymbol{k}}, \quad T i T^{-1} = -i, \quad T H_i T^{-1} = H_i. \quad \text{(B1)}$$

Note that T is not equivalent to the physical time-reversal $\mathcal{T}$ defined earlier in Eq. (3.18), which always leaves H_ψ invariant. Rather, as we show below, T leaves the Hamiltonian invariant only if the Higgs condensate is absent.

Under T, we find the following transformation of the Hamiltonian H_ψ:

$$T H_\psi T^{-1} = H_\psi - \sum_{\boldsymbol{k}} \chi_{\boldsymbol{k},s}^\dagger \hat{\Theta}_{s,s'} \chi_{\boldsymbol{k},s'}, \quad \text{where } \hat{\Theta} = 2 \begin{pmatrix} \Theta^z & \Theta^- \\ \Theta^+ & -\Theta^z \end{pmatrix} = 2 \Theta^b \tau^b. \quad \text{(B2)}$$

Therefore, the Hamiltonian H_ψ commutes with T when $\hat{\Theta} = 0$. One can also show that the charge current operator $J_\rho(i)$ is odd under T, i.e,

$$T J_\rho(i) T^{-1} = -J_\rho(i). \quad \text{(B3)}$$

Therefore, when $\hat{\Theta} = 0$, we can use the symmetry of H_ψ under T to find that:

$$\langle J_\rho(i) \rangle = \langle T J_\rho(i) T^{-1} \rangle = -\langle J_\rho(i) \rangle \implies \langle J_\rho(i) \rangle = 0. \quad \text{(B4)}$$

The physical content of the above equation is that current loop order cannot arise if all the SU(2) gauge bosons are deconfined, but can possibly arise when a Higgs condensate reduces the gauge group to U(1) or $\mathbb{Z}_2$.

Appendix C: Real space perturbation theory for current in presence of large Higgs field

We consider the limit where the Higgs field $H^a(i)$ is much larger compared to the hopping matrix elements of the $\psi_\pm$ fermions, characterized by $w_\rho U_{i,i+\boldsymbol{v}_\rho}$. In the $|H_i| \to \infty$ limit, the Hamiltonian has only on-site terms, and therefore there is no current on the links. In this section, we perform a perturbation series expansion in $1/|H_i|$ to find an expression for the current. Recall that the charge gap of the SU(2) lattice gauge theory is determined by $|H_i|$, and so this is similar to a $1/U$ expansion in the underlying Hubbard model.

We define a lattice Green's function in imaginary time in the standard fashion:

$$G_{ij}(\tau) = -\langle T_\tau (\psi_i(\tau)\psi_j^\dagger(0))\rangle. \tag{C1}$$

The Matsubara Green's function in the bare limit, $G_{i,n}^0$ is diagonal in real space (we set $\lambda = -1$):

$$G_{i,n}^0 = (i\omega_n - H_i^a \sigma^a)^{-1} = \frac{i\omega_n + H_i^a \sigma^a}{(i\omega_n)^2 - H_i^2}. \tag{C2}$$

where we have set $\mu = 0$ for convenience (it does not modify our conclusion). The Dyson equation for the Green's function in real space is given by:

$$
\begin{aligned}
G_{ij,n} &= G_{i,n}^0 \delta_{ij} + \sum_k G_{i,n}^0 w_{ki} U_{ki} G_{kj,n} \\
&= G_{i,n}^0 \delta_{ij} + G_{i,n}^0 w_{ji} U_{ji} G_{j,n}^0 + \sum_k G_{i,n}^0 w_{ki} U_{ki} G_{k,n}^0 w_{jk} U_{jk} G_{j,n}^0 + ... \\
&\equiv G_{i,n}^0 \delta_{ij} + G_{ij,n}^{(1)} + G_{ij,n}^{(2)} + ...
\end{aligned}
\tag{C3}
$$

where $w_{ij} = w_\rho$ is the hopping along the link $\langle i,j \rangle = \langle i, i + \boldsymbol{v}_\rho \rangle$. Recall that the current operator on the link $\langle i, i + \boldsymbol{v}_\rho \rangle$ is given by:

$$J_{i,i+\boldsymbol{v}_\rho} = -i\boldsymbol{v}_\rho w_\rho \left(\psi_i^\dagger U_{i,i+\boldsymbol{v}_\rho} \psi_{i+\boldsymbol{v}_\rho} - \text{H.c.} \right). \tag{C4}$$

Therefore, we can write the its expectation value in terms of the Green's function defined above as follows:

$$\langle J_{i,i+\boldsymbol{v}_\rho} \rangle = -i\boldsymbol{v}_\rho w_\rho \left[\text{Tr}(U_{i,i+\boldsymbol{v}_\rho} G_{i+\boldsymbol{v}_\rho,i}) - \text{Tr}(U_{i+\boldsymbol{v}_\rho,i} G_{i,i+\boldsymbol{v}_\rho}) \right] (\tau \to 0^-). \tag{C5}$$

The lowest order term in $1/|H_i|$ corresponds to $G_{ij} = G_i^0 \delta_{ij}$, which gives zero current consistent with our expectations. To the next order in $1/|H_i|$, we find that the forward and backward currents exactly cancel and therefore the current is equal to zero to this order as well (via the cyclic property of the trace).

$$
\begin{aligned}
\langle J_{i,i+\boldsymbol{v}_\rho}^{(1)} \rangle &= -i\boldsymbol{v}_\rho w_\rho \left[\text{Tr}(U_{i,i+\boldsymbol{v}_\rho} G_{i+\boldsymbol{v}_\rho,i}^{(1)}) - \text{Tr}(U_{i+\boldsymbol{v}_\rho,i} G_{i,i+\boldsymbol{v}_\rho}^{(1)}) \right] \\
&= -i\boldsymbol{v}_\rho w_\rho \left[\text{Tr}(U_{i,i+\boldsymbol{v}_\rho} G_{i+\boldsymbol{v}_\rho}^0 U_{i+\boldsymbol{v}_\rho} G_i^0) - \text{Tr}(U_{i+\boldsymbol{v}_\rho,i} G_i^0 U_{i,i+\boldsymbol{v}_\rho} G_{i+\boldsymbol{v}_\rho}^0) \right] = 0.
\end{aligned}
\tag{C6}
$$

This exemplifies the importance of requiring non-nearest neighbor coupling for a non-zero current on the nearest neighbor bonds, albeit in a large Higgs field limit.

The next term in the perturbation series, coming from $G^{(2)}$, gives us a non-zero current. To be more specific, let us label the sites as in Fig. 4, and compute the current from m to j. It involves all triangles consisting of m, j and a third site connected to both by a non-zero hopping (for simplicity we consider only nearest neighbor and next nearest neighbor hoppings).

$$\langle \boldsymbol{J}_{j,m}^{(2)}\rangle = i\boldsymbol{v}_{jm}w_1^2 w_2 \, \mathrm{Tr}\left[U_{jm}G_m^0\left(U_{ml}G_l^0 U_{lj} + U_{mi}G_i^0 U_{ij} + U_{mn}G_n^0 U_{nj} + U_{mk}G_k^0 U_{kj}\right)G_j^0\right]$$
$$-i\boldsymbol{v}_{jm}w_1^2 w_2 \, \mathrm{Tr}\left[U_{mj}G_j^0\left(U_{jl}G_l^0 U_{lm} + U_{ji}G_i^0 U_{im} + U_{jn}G_n^0 U_{nm} + U^{jk}G_k^0 U_{km}\right).G_m^0\right] \; \text{(C7)}$$

where w_1, w_2 are the nearest and next nearest neighbor hopping respectively. Note that the second term is just the Hermitian conjugate of the first term. We now convert to Matsubara Green's functions and evaluate the frequency summation (for simplicity we assume that H_i are different on each site). The eigenstates at site i have energy $\pm|H_i|$, therefore in the $T = 0$ limit only the negative energy eigenstates contribute to the current.

Since the contribution of all triangular plaquettes to the current are similar, we only evaluate the contributions to the current by the first term in Eq. (C7) and its Hermitian conjugate (corresponding to the triangular plaquette $\triangle_{jlm}$).

$$\frac{1}{\beta}\left(\sum_{i\omega_n}\mathrm{Tr}\left[U_{jm}G_m^0 U_{ml}G_l^0 U_{lj}G_j^0\right] - \mathrm{Tr}\left[U_{jm}G_m^0 U_{ml}G_l^0 U_{lj}G_j^0\right]\right) =$$
$$\mathrm{Tr}\left[U_{jm}\left(\frac{-|H_m| + H_m^a\sigma^a}{-2|H_m|}\right)U_{ml}\left(\frac{-|H_m| + H_l^a\sigma^a}{H_m^2 - H_l^2}\right)U_{lj}\left(\frac{-|H_m| + H_j^a\sigma^a}{H_m^2 - H_j^2}\right)\right]$$
$$+ (j \to m \to l \to j) + (j \to l \to m \to j) - \text{H.c.} \quad \text{(C8)}$$

Using the unitarity of U and $U_{\alpha\beta} = U_{\beta\alpha}^\dagger$, we can show quite generally that $\mathrm{Tr}(U_{jm}U_{ml}U_{lj}) = \mathrm{Tr}(U_{jl}U_{lm}U_{mj})$, so the term without any Higgs field $H_\alpha^a\sigma^a$ for some site α cancels with the contribution from the second line in Eq. (C7). The terms with two Higgs fields of the form $H_\alpha^a\sigma^a$ also cancel out with their Hermitian conjugates for the same reason. Therefore, we are left with two kinds of terms, both of which fall off as $|H_i|^{-2}$. The contribution to the current from this particular triangular plaquette can be written as:

$$J_{\triangle_{jlm}} \sim i\left[\left(H_m^a\,\mathrm{Tr}(U_{jm}\sigma^a U_{ml}U_{lj}) + H_l^a\,\mathrm{Tr}(U_{jm}U_{ml}\sigma^a U_{lj}) + H_j^a\,\mathrm{Tr}(U_{jm}U_{ml}U_{lj}\sigma^a)\right)f(|H|) +\right.$$
$$\left. H_m^a H_l^b H_j^c\,\mathrm{Tr}(U_{jm}\sigma^a U_{ml}\sigma^b U_{lj}\sigma^c)g(|H|) - \text{H.c.}\right], \quad \text{(C9)}$$

where $f(|H|)$ and $g(|H|)$ are scalar functions of the Higgs fields (invariant under all symmetry

operations), given by:

$$f(|H|) = \frac{1}{2(|H_m| + |H_l|)(|H_m| + |H_j|)(|H_m| + |H_l|)}$$

$$g(|H|) = -\frac{|H_m| + |H_l| + |H_j|}{2|H_m||H_l||H_j|(|H_m| + |H_l|)(|H_m| + |H_j|)(|H_m| + |H_l|)}. \tag{C10}$$

We chose a particular set of terms, coming from $\triangle_{jlm}$ and the three other triangles related to it by reflection symmetries, as our order parameter O_{jm} in Fig. 4. The other three contributions to the current on the link $\langle j, m \rangle$ in Eq. (C7) may be obtained by replacing the third vertex l of the triangle by that of the triangle under consideration (i, k and n). The net result for the current therefore contains the expressions presented in Fig. 4, along with three other expressions which can also serve as valid representations of $\boldsymbol{O}$.

---

[1] Y. Ando, K. Segawa, S. Komiya, and A. N. Lavrov, "Electrical Resistivity Anisotropy from Self-Organized One Dimensionality in High-Temperature Superconductors," Phys. Rev. Lett. **88**, 137005 (2002), cond-mat/0108053.

[2] B. Fauqué, Y. Sidis, V. Hinkov, S. Pailhès, C. T. Lin, X. Chaud, and P. Bourges, "Magnetic Order in the Pseudogap Phase of High-T_c Superconductors," Phys. Rev. Lett. **96**, 197001 (2006), cond-mat/0509210.

[3] V. Hinkov, D. Haug, B. Fauqué, P. Bourges, Y. Sidis, A. Ivanov, C. Bernhard, C. T. Lin, and B. Keimer, "Electronic Liquid Crystal State in the High-Temperature Superconductor $YBa_2Cu_3O_{6.45}$," Science **319**, 597 (2008).

[4] Y. Li, V. Balédent, N. Barišić, Y. Cho, B. Fauqué, Y. Sidis, G. Yu, X. Zhao, P. Bourges, and M. Greven, "Unusual magnetic order in the pseudogap region of the superconductor $HgBa_2CuO_{4+\delta}$," Nature **455**, 372 (2008), arXiv:0805.2959 [cond-mat.supr-con].

[5] J. Xia, E. Schemm, G. Deutscher, S. A. Kivelson, D. A. Bonn, W. N. Hardy, R. Liang, W. Siemons, G. Koster, M. M. Fejer, and A. Kapitulnik, "Polar Kerr-Effect Measurements of the High-Temperature $YBa_2Cu_3O_{6+x}$ Superconductor: Evidence for Broken Symmetry near the Pseudogap Temperature," Phys. Rev. Lett. **100**, 127002 (2008), arXiv:0711.2494 [cond-mat.supr-con].

[6] R. Daou, J. Chang, D. Leboeuf, O. Cyr-Choinière, F. Laliberté, N. Doiron-Leyraud, B. J. Ramshaw, R. Liang, D. A. Bonn, W. N. Hardy, and L. Taillefer, "Broken rotational symmetry in the pseudogap phase of a high-T_c superconductor," Nature **463**, 519 (2010), arXiv:0909.4430 [cond-mat.supr-con].

[7] Y. Li, V. Balédent, G. Yu, N. Barišić, K. Hradil, R. A. Mole, Y. Sidis, P. Steffens, X. Zhao, P. Bourges, and M. Greven, "Hidden magnetic excitation in the pseudogap phase of a high-T_c superconductor," Nature **468**, 283 (2010), arXiv:1007.2501 [cond-mat.supr-con].

[8] M. J. Lawler, K. Fujita, J. Lee, A. R. Schmidt, Y. Kohsaka, C. K. Kim, H. Eisaki, S. Uchida, J. C. Davis, J. P. Sethna, and E.-A. Kim, "Intra-unit-cell electronic nematicity of the high-T_c copper-oxide pseudogap states," Nature **466**, 347 (2010), arXiv:1007.3216 [cond-mat.supr-con].

[9] Y. Lubashevsky, L. Pan, T. Kirzhner, G. Koren, and N. P. Armitage, "Optical Birefringence and Dichroism of Cuprate Superconductors in the THz Regime," Phys. Rev. Lett. **112**, 147001 (2014), arXiv:1310.2265 [cond-mat.str-el].

[10] L. Mangin-Thro, Y. Sidis, A. Wildes, and P. Bourges, "Intra-unit-cell magnetic correlations near optimal doping in $YBa_2Cu_3O_{6.85}$," Nature Communications **6**, 7705 (2015), arXiv:1501.04919 [cond-mat.supr-con].

[11] L. Zhao, D. H. Torchinsky, H. Chu, V. Ivanov, R. Lifshitz, R. Flint, T. Qi, G. Cao, and D. Hsieh, "Evidence of an odd-parity hidden order in a spin-orbit coupled correlated iridate," Nature Physics **12**, 32 (2016), arXiv:1601.01688 [cond-mat.str-el].

[12] L. Zhao, C. A. Belvin, R. Liang, D. A. Bonn, W. N. Hardy, N. P. Armitage, and D. Hsieh, "A global inversion-symmetry-broken phase inside the pseudogap region of $YBa_2Cu_3O_y$," Nature Physics **13**, 250 (2017), arXiv:1611.08603 [cond-mat.str-el].

[13] J. Jeong, Y. Sidis, A. Louat, V. Brouet, and P. Bourges, "Time-reversal symmetry breaking hidden order in $Sr_2(Ir,Rh)O_4$," Nature Communications **8**, 15119 (2017), arXiv:1701.06485 [cond-mat.str-el].

[14] S. A. Kivelson, E. Fradkin, and V. J. Emery, "Electronic liquid-crystal phases of a doped Mott insulator," Nature **393**, 550 (1998).

[15] C. M. Varma, "Non-Fermi-liquid states and pairing instability of a general model of copper oxide metals," Phys. Rev. B **55**, 14554 (1997), cond-mat/9607105.

[16] M. E. Simon and C. M. Varma, "Detection and Implications of a Time-Reversal Breaking State in Underdoped Cuprates," Phys. Rev. Lett. **89**, 247003 (2002), cond-mat/0201036.

[17] M. E. Simon and C. M. Varma, "Symmetry considerations for the detection of second-harmonic generation in cuprates in the pseudogap phase," Phys. Rev. B **67**, 054511 (2003), cond-mat/0210672.

[18] F. Wang and T. Senthil, "Twisted Hubbard Model for Sr_2IrO_4: Magnetism and Possible High Temperature Superconductivity," Phys. Rev. Lett. **106**, 136402 (2011), arXiv:1011.3500 [cond-mat.str-el].

[19] J. A. Hertz, "Quantum critical phenomena," Phys. Rev. B **14**, 1165 (1976).

[20] A. V. Chubukov and S. Sachdev, "Chubukov and Sachdev reply," Phys. Rev. Lett. **71**, 3615 (1993).

[21] T. Senthil, S. Sachdev, and M. Vojta, "Fractionalized Fermi Liquids," Phys. Rev. Lett. **90**, 216403 (2003), cond-mat/0209144.

[22] T. Senthil, M. Vojta, and S. Sachdev, "Weak magnetism and non-Fermi liquids near heavy-fermion critical points," Phys. Rev. B **69**, 035111 (2004), cond-mat/0305193.

[23] A. Paramekanti and A. Vishwanath, "Extending Luttinger's theorem to $\mathbb{Z}_2$ fractionalized phases of matter," Phys. Rev. B **70**, 245118 (2004), cond-mat/0406619.

24 M. Punk, A. Allais, and S. Sachdev, "Quantum dimer model for the pseudogap metal," Proc Nat. Acad. Sci **112**, 9552 (2015), arXiv:1501.00978 [cond-mat.str-el].

25 M. Punk and S. Sachdev, "Fermi surface reconstruction in hole-doped t-J models without long-range antiferromagnetic order," Phys. Rev. B **85**, 195123 (2012), arXiv:1202.4023 [cond-mat.str-el].

26 Topological order is defined by the presence of ground state degeneracy of a system on a torus. More precisely, on a torus of size L, the lowest energy states have an energy difference which is of order $\exp(-\alpha L)$ for some constant α. Topological order can also be present in gapless states, including those with Fermi surfaces.[21,22] In such states, the non-topological gapless excitations have an energy of order $1/L^z$ (for some positive z) above the ground state on the torus, and so can be distinguished from the topologically degenerate states. Topological order is required for metals to have a Fermi surface volume distinct from the Luttinger volume,[22] and hence to have a 'pseudogap'.

27 S. Sachdev and D. Chowdhury, "The novel metallic states of the cuprates: Fermi liquids with topological order and strange metals," Prog. Theor. Exp. Phys. **2016**, 12C102 (2016), arXiv:1605.03579 [cond-mat.str-el].

28 N. Read and S. Sachdev, "Large N expansion for frustrated quantum antiferromagnets," Phys. Rev. Lett. **66**, 1773 (1991).

29 S. Sachdev and N. Read, "Large N expansion for frustrated and doped quantum antiferromagnets," Int. J. Mod. Phys. B **5**, 219 (1991), cond-mat/0402109.

30 M. Barkeshli, H. Yao, and S. A. Kivelson, "Gapless spin liquids: Stability and possible experimental relevance," Phys. Rev. B **87**, 140402 (2013), arXiv:1208.3869 [cond-mat.str-el].

31 S. Sachdev, M. A. Metlitski, Y. Qi, and C. Xu, "Fluctuating spin density waves in metals," Phys. Rev. B **80**, 155129 (2009), arXiv:0907.3732 [cond-mat.str-el].

32 D. Chowdhury and S. Sachdev, "Higgs criticality in a two-dimensional metal," Phys. Rev. B **91**, 115123 (2015), arXiv:1412.1086 [cond-mat.str-el].

33 S. Chakravarty, B. I. Halperin, and D. R. Nelson, "Low-temperature behavior of two-dimensional quantum antiferromagnets," Phys. Rev. Lett. **60**, 1057 (1988).

34 S. Chakravarty, B. I. Halperin, and D. R. Nelson, "Two-dimensional quantum Heisenberg antiferromagnet at low temperatures," Phys. Rev. B **39**, 2344 (1989).

35 F. D. M. Haldane, "O(3) Nonlinear σ Model and the Topological Distinction between Integer- and Half-Integer-Spin Antiferromagnets in Two Dimensions," Phys. Rev. Lett. **61**, 1029 (1988).

36 N. Read and S. Sachdev, "Valence-bond and spin-Peierls ground states of low-dimensional quantum antiferromagnets," Phys. Rev. Lett. **62**, 1694 (1989).

37 N. Read and S. Sachdev, "Spin-Peierls, valence-bond solid, and Néel ground states of low-dimensional quantum antiferromagnets," Phys. Rev. B **42**, 4568 (1990).

38 T. Senthil, A. Vishwanath, L. Balents, S. Sachdev, and M. P. A. Fisher, "Deconfined Quantum Critical

Points," Science **303**, 1490 (2004), cond-mat/0311326.

39 T. Senthil, L. Balents, S. Sachdev, A. Vishwanath, and M. P. A. Fisher, "Quantum criticality beyond the Landau-Ginzburg-Wilson paradigm," Phys. Rev. B **70**, 144407 (2004), cond-mat/0312617.

40 D. Bohm, "Note on a Theorem of Bloch Concerning Possible Causes of Superconductivity," Phys. Rev. **75**, 502 (1949).

41 Y. Ohashi and T. Momoi, "On the Bloch Theorem Concerning Spontaneous Electric Current," J. Phys. Soc. Jpn. **65**, 3254 (1996), cond-mat/9606182.

42 T. D. Stanescu and P. Phillips, "Nonperturbative approach to full Mott behavior," Phys. Rev. B **69**, 245104 (2004), cond-mat/0301254.

43 E. Berg, C.-C. Chen, and S. A. Kivelson, "Stability of Nodal Quasiparticles in Superconductors with Coexisting Orders," Phys. Rev. Lett. **100**, 027003 (2008), arXiv:0710.0113 [cond-mat.supr-con].

44 S. Sachdev, E. Berg, S. Chatterjee, and Y. Schattner, "Spin density wave order, topological order, and Fermi surface reconstruction," Phys. Rev. B **94**, 115147 (2016), arXiv:1606.07813 [cond-mat.str-el].

45 Y. Yoshida, S. Schröder, P. Ferriani, D. Serrate, A. Kubetzka, K. von Bergmann, S. Heinze, and R. Wiesendanger, "Conical Spin-Spiral State in an Ultrathin Film Driven by Higher-Order Spin Interactions," Phys. Rev. Lett. **108**, 087205 (2012).

46 M. Hermele, T. Senthil, M. P. A. Fisher, P. A. Lee, N. Nagaosa, and X.-G. Wen, "Stability of U (1) spin liquids in two dimensions," Phys. Rev. B **70**, 214437 (2004), cond-mat/0404751.

47 R. K. Kaul, Y. B. Kim, S. Sachdev, and T. Senthil, "Algebraic charge liquids," Nature Physics **4**, 28 (2008), arXiv:0706.2187 [cond-mat.str-el].

48 X. G. Wen, "Mean-field theory of spin-liquid states with finite energy gap and topological orders," Phys. Rev. B **44**, 2664 (1991).

49 R. K. Kaul, A. Kolezhuk, M. Levin, S. Sachdev, and T. Senthil, "Hole dynamics in an antiferromagnet across a deconfined quantum critical point," Phys. Rev. B **75**, 235122 (2007), cond-mat/0702119.

50 R. K. Kaul, M. A. Metlitski, S. Sachdev, and C. Xu, "Destruction of Néel order in the cuprates by electron doping," Phys. Rev. B **78**, 045110 (2008), arXiv:0804.1794 [cond-mat.str-el].

51 R. M. Fernandes and A. V. Chubukov, "Low-energy microscopic models for iron-based superconductors: a review," Rep. Prog. Phys. **80**, 014503 (2017), arXiv:1607.00865 [cond-mat.str-el].

52 S. Badoux, W. Tabis, F. Laliberté, G. Grissonnanche, B. Vignolle, D. Vignolles, J. Béard, D. A. Bonn, W. N. Hardy, R. Liang, N. Doiron-Leyraud, L. Taillefer, and C. Proust, "Change of carrier density at the pseudogap critical point of a cuprate superconductor," Nature **531**, 210 (2016), arXiv:1511.08162 [cond-mat.supr-con].

53 R. A. Cooper, Y. Wang, B. Vignolle, O. J. Lipscombe, S. M. Hayden, Y. Tanabe, T. Adachi, Y. Koike, M. Nohara, H. Takagi, C. Proust, and N. E. Hussey, "Anomalous Criticality in the Electrical Resistivity of $La_{2-x}Sr_xCuO_4$," Science **323**, 603 (2009).

[54] I. Božović, X. He, J. Wu, and A. T. Bollinger, "Dependence of the critical temperature in overdoped copper oxides on superfluid density," Nature **536**, 309 (2016).

[55] X.-G. Wen, "Quantum orders and symmetric spin liquids," Phys. Rev. B **65**, 165113 (2002), cond-mat/0107071.

[56] A. V. Chubukov, T. Senthil, and S. Sachdev, "Universal magnetic properties of frustrated quantum antiferromagnets in two dimensions," Phys. Rev. Lett. **72**, 2089 (1994), cond-mat/9311045.

[57] S. Sachdev, "Colloquium: Order and quantum phase transitions in the cuprate superconductors," Rev. Mod. Phys. **75**, 913 (2003), cond-mat/0211005.

[58] T. Senthil and M. P. A. Fisher, "$\mathbb{Z}_2$ gauge theory of electron fractionalization in strongly correlated systems," Phys. Rev. B **62**, 7850 (2000), cond-mat/9910224.

[59] L. Balents and S. Sachdev, "Dual vortex theory of doped Mott insulators," Annals of Physics **322**, 2635 (2007), cond-mat/0612220.

[60] S. Chatterjee, Y. Qi, S. Sachdev, and J. Steinberg, "Superconductivity from a confinement transition out of a fractionalized Fermi liquid with Z_2 topological and Ising-nematic orders," Phys. Rev. B **94**, 024502 (2016), arXiv:1603.03041 [cond-mat.str-el].

[61] A. Eberlein, W. Metzner, S. Sachdev, and H. Yamase, "Fermi Surface Reconstruction and Drop in the Hall Number due to Spiral Antiferromagnetism in High-T_c Cuprates," Phys. Rev. Lett. **117**, 187001 (2016), arXiv:1607.06087 [cond-mat.str-el].

[62] S. Chatterjee, S. Sachdev, and A. Eberlein, "Thermal and electrical transport in metals and superconductors across antiferromagnetic and topological quantum transitions," (2017), arXiv:1704.02329 [cond-mat.str-el].

[63] F. Laliberte, W. Tabis, S. Badoux, B. Vignolle, D. Destraz, N. Momono, T. Kurosawa, K. Yamada, H. Takagi, N. Doiron-Leyraud, C. Proust, and L. Taillefer, "Origin of the metal-to-insulator crossover in cuprate superconductors," ArXiv e-prints (2016), arXiv:1606.04491 [cond-mat.supr-con].

[64] C. Collignon, S. Badoux, S. A. A. Afshar, B. Michon, F. Laliberte, O. Cyr-Choiniere, J.-S. Zhou, S. Licciardello, S. Wiedmann, N. Doiron-Leyraud, and L. Taillefer, "Fermi-surface transformation across the pseudogap critical point of the cuprate superconductor $La_{1.6-x}Nd_{0.4}Sr_xCuO_4$," ArXiv e-prints (2016), arXiv:1607.05693 [cond-mat.supr-con].

[65] B. M. Michon, S. Li, P. Bourgeois-Hope, S. Badoux, J.-S. Zhou, N. Doiron-Leyraud, and L. Taillefer, "Pseudogap critical point inside the superconducting phase of a cuprate : a thermal conductivity study in Nd-LSCO," unpublished (2017).